PUCRS

FACULDADE DE BIOCIÊNCIAS
PROGRAMA DE PÓS-GRADUAÇÃO EM BIOLOGIA CELULAR E MOLECULAR
MESTRADO EM BIOLOGIA CELULAR E MOLECULAR

PEDRO FERRARI DALBERTO

CARACTERIZAÇÃO BIOQUÍMICA E ESTRUTURAL DA ENZIMA INOSINA-URIDINA NUCLEOSÍDEO HIDROLASE DE *LEISHMANIA BRAZILIENSIS*

Porto Alegre

2017

PÓS-GRADUAÇÃO - *STRICTO SENSU*

Pontifícia Universidade Católica
do Rio Grande do Sul

Pedro Ferrari Dalberto

CARACTERIZAÇÃO BIOQUÍMICA E ESTRUTURAL DA ENZIMA INOSINA-URIDINA NUCLEOSÍDEO HIDROLASE DE *LEISHMANIA BRAZILIENSIS*

Dissertação de Mestrado apresentada ao Programa de Pós-Graduação em Biologia Celular e Molecular da Pontifícia Universidade Católica do Rio Grande do Sul.

Orientador: Prof. Dr. Diógenes Santiago Santos

Coorientador: Dra. Anne Drumond Villela

Porto Alegre

2017

Ficha Catalográfica

Ficha Catalográfica

D137c Dalberto, Pedro Ferrari

Caracterização Bioquímica e Estrutural da Enzima Inosina-Uridina Hidrolase de Leishmania brasiliensis / Pedro Ferrari Dalberto . – 2017.
65 f.
Dissertação (Mestrado) – Programa de Pós-Graduação em Biologia Celular e Molecular, PUCRS.

Orientador: Prof. Dr. Diógenes Santiago Santos.
Co-orientadora: Dra. Anne Drumond Villela.

1. Protozoário. 2. Leishmania. 3. Salvamento de Purinas. 4. Hidrolase. 5. IU-NH. I. Santos, Diógenes Santiago. II. Villela, Anne Drumond. III. Título.

Elaborada pelo Sistema de Geração Automática de Ficha Catalográfica da PUCRS com os dados fornecidos pelo(a) autor(a).

Pedro Ferrari Dalberto

Caracterização Bioquímica e Estrutural da Enzima Inosina-Uridina Nucleosídeo Hidrolase de *Leishmania braziliensis*

Dissertação de Mestrado apresentada ao Programa de Pós-Graduação em Biologia Celular e Molecular, da Faculdade de Biociências da Pontifícia Universidade Católica do Rio Grande do Sul.

Aprovado em _____de_____de_____

BANCA EXAMINADORA

_____

Profa. Dra. Carla Denise Bonan - PUCRS

_____

Profa. Dra. Denise Cantarelli Machado - PUCRS

_____

Prof. Dr. Diogo Onofre Gomes de Souza - UFRGS

Porto Alegre

2017

AGRADECIMENTOS

Gostaria de agradecer, primeiramente, ao meu orientador professor Dr. Diógenes Santiago Santos pela oportunidade de fazer parte do Centro de Pesquisas em Biologia Molecular e Funcional/Instituto Nacional de Ciência e Tecnologia em Tuberculose (CPBMF/INCT), bem como a confiança e apoio durante estes anos e por todos ensinamentos que foram fundamentais em todas as etapas deste trabalho.

À minha coorientadora, Dra. Anne Drumond Villela, pela paciência, apoio e dedicação por todos os anos que trabalhamos juntos. Sempre me orientando em busca de conhecimento científico e me incentivando a melhorar.

Ao professor Dr. Luiz Augusto Basso, pela paciência e dedicação nas discussões dos resultados.

Ao Dr. Leonardo Kras Borges Martinelli por todo o ensino, pela ajuda na realização dos experimentos e pelas discussões dos resultados.

Aos meus colegas, Dr. Antônio Frederico Michel Pinto, Dr. Valnês Rodrigues Junior, Dr. Guilherme Petersen e Me. Adílio Dadda, pela amizade e apoio.

Aos demais colegas e ex-colegas do CPBFM que de alguma forma me ajudaram na realização deste trabalho.

Aos meus pais pela estrutura e apoio durante estes anos.

RESUMO

A leishmaniose é considerada uma das principais doenças endêmicas do mundo e o Brasil está entre os países com a maior incidência das formas cutâneas e mucocutâneas de leishmaniose causadas principalmente pela *Leishmania braziliensis*. Embora o tratamento desta doença esteja disponível, os fármacos de primeira linha contra a leishmaniose possuem várias limitações: administração parenteral, longa duração do tratamento e muitos efeitos adversos. Uma das principais características metabólicas destes parasitas é a ausência da via de biossíntese *de novo* de purinas, tornando-os dependentes unicamente da via de salvamento para a síntese de nucleotídeos. A melhor compreensão da via de salvamento de purinas pode revelar detalhes da biologia de *L. braziliensis* que, por sua vez, podem ser usadas para desenvolver novas estratégias para combater este parasita. A Inosina-Uridina Nucleosídeo Hidrolase de *L. braziliensis* (*Lb*IU-NH) desempenha um papel importante na rota de salvamento e é um alvo molecular interessante para o desenvolvimento de novos fármacos, uma vez que não existe uma atividade catalítica semelhante em mamíferos. Neste trabalho, descrevemos a clonagem, expressão e a purificação da proteína recombinante homogênea. A determinação das constantes cinéticas da *Lb*IU-NH no estado estacionário para inosina, adenosina, citidina e uridina foram determinadas. Estes dados sugerem funções e características distintas de uma hidrolase não específica. O perfil termodinâmico sugere que apenas a ribose pode ligar à enzima livre com contribuições tanto entalpica (ΔH) quanto entrópica (ΔS) favoráveis. Os parâmetros de ativação termodinâmica (Ea, $\Delta G^{\#}$, $\Delta S^{\#}$, $\Delta H^{\#}$) para a reação catalisada pela *Lb*IU-NH, cinética no estado pré-estacionário, efeito isótopico do solvente e perfil de pH também foram determinados. Além disso, descrevemos a estrutura cristalina de *Lb*IU-NH complexada com ribose e Ca^{2+} a 1.5 Å de resolução.

ABSTRACT

Leishmaniasis is considered one of the main endemic diseases in the world, and Brazil is among the countries, which has the highest incidence of cutaneous and mucocutaneous forms of leishmaniosis caused mainly by *Leishmania braziliensis*. Although the treatment of this disease is available, the first-line drugs against leishmaniosis have several limitations: parenteral administration, long duration of treatment, and serious toxicities. One key metabolic characteristic of this parasite is the lack of purine *de novo* biosynthesis pathway, relying only on the purine salvage pathway for nucleotide synthesis. The better understanding of the purine salvage pathway can reveal details of the biology of *L. braziliensis* that could be used to develop new strategies to combat this parasite. The inosine-uridine nucleoside hydrolase from *L. braziliensis* (*Lb*IU-NH) plays an important role in the salvage process and is an attractive drug target as there is no similar catalytic activity in mammals. Here, it is described the cloning, expression, and purification of the homogenous recombinant protein. Determination of *Lb*IU-NH steady-state kinetic constants for inosine, adenosine, cytidine and uridine are reported. These data suggest distinct functions and characteristics of a nonspecific hydrolase. Thermodynamic profile suggests that only ribose can bind to free enzyme with favorable enthalpic (ΔH) and entropic (ΔS) contributions. Thermodynamic activation parameters (E_a, $\Delta G^{\#}$, $\Delta S^{\#}$, $\Delta H^{\#}$) for the *Lb*IU-NH-catalyzed chemical reaction, pre-steady-state kinetics, solvent kinetic isotope effects, and pH-rate profiles are also presented. In addition, the crystal structure of *Lb*IU-NH in complex with ribose and Ca^{2+} at 1.5 Å resolution is described.

SUMÁRIO

Capítulo 1

Capítulo 2

Capítulo 3

Capítulo 1

Introdução

Justificativa

Objetivos

1. INTRODUÇÃO

1.1 A LEISHMANIOSE

A leishmaniose é uma doença infecciosa e não contagiosa, cujos agentes etiológicos são protozoários pertencentes à família Trypanosomatidae, do gênero *leishmania*.[1,2] Estes parasitas são encontrados em quase todos continentes, exceto na Oceania, e mais de 20 espécies já foram descobertas. No Brasil, foram identificadas sete espécies de *Leishmania*, sendo seis do subgênero *Viannia* e uma do subgênero *Leishmania.*[3] As espécies *Leishmania* (*Vianna*) *braziliensis*, *Leishmania* (*V*.) *guyanensis e Leishmania* (*Leishmania*) *amazonensis* ganham destaque, pois são as principais causadoras da Leishmaniose Tegumentar Americana no país.[3,4]

A leishmaniose é caracterizada pela Organização Mundial da Saúde (OMS) como uma das seis principais doenças endêmicas no mundo em que o número de casos está aumentando.[1] A epidemiologia da leishmaniose depende das características das espécies dos parasitas, das condições socioeconômicas da região, da mobilidade e das mudanças ambientais e climáticas dos locais de transmissão.[1,2,4] A doença pode se manifestar de três principais formas:

- Leishmaniose visceral (LV): Conhecida como Calazar, caracteriza-se por episódios de febre, perda de peso, aumento do baço e do fígado, e anemia.[5-7] Estima-se que 200 000 a 400 000 novos casos ocorrem no mundo a cada ano e que mais de 90% dos novos casos relatados à OMS ocorreram em seis países no ano de 2015: Brasil, Etiópia, Índia, Somália, Sudão e Sudão do Sul;[5]

- Leishmaniose cutânea (LC): É a forma mais comum de leishmaniose e causa lesões cutâneas, principalmente úlceras, em partes expostas do corpo, deixando cicatrizes.[1,8,9] Cerca de 0,7 a 1,3 milhão de novos casos ocorrem anualmente em todo o mundo, sendo que 95% dos novos casos estão concentrados no Brasil, Afeganistão, Argélia, Colômbia e Irã no ano de 2015;[5]

- Leishmania mucocutânea: Na maioria dos casos é uma evolução secundária da forma cutânea e é caracterizada por lesões na face que levam a destruição parcial ou total das membranas mucosas do nariz, boca e garganta.[1,3,9,10] Em 2015, aproximadamente 90% dos casos de leishmaniose mucocotânea ocorreram no Brasil, Bolívia e Peru.[5]

No Brasil, predominam as formas de LC e mucocutânea causadas principalmente pela *L. braziliensis* que é encontrada em todas a regiões do país.[5,11,12] Segundo o Ministério da Saúde, no ano de 2015, ocorreram aproximadamente 20 mil casos de LC e cerca de 3,2 mil casos de LV, sendo as regiões norte e nordeste as mais afetadas.[12]

1.2 O VETOR

A doença é transmitida através de mosquitos flebotomídeos (Ordem Diptera; Família Psychodidae; Sub-Família Phlebtominae), que ingerem junto com o sangue as formas amastigotas de um animal infectado que se transformam em promastigotas (forma alongada com flagelo). No intestino de seus vetores, multiplicam-se e migram para proboscíde do inseto e em menos de cinco dias podem ser inoculados na pele do hospedeiro vertebrado.[13] Em todo o mundo são conhecidas aproximadamente 900 espécies de flebomídeos.[14] No Brasil, são conhecidos popularmente como mosquito palha, tatuquira e birigui, possuem pernas longas e delgadas, coloração castanho-claro e eles não passam de 0.5 cm de comprimento.[3,4] O papel vetorial de cada espécie do mosquito dependerá da espécie de *Leishmania* presente no intestino do vetor.[3]

1.3 CICLO DE TRANSMISSÃO

O ciclo de transmissão inicia quando a fêmea de flebotomíneos ingere sangue do hospedeiro que contém macrófagos contendo leishmanias na forma amastigota. Estas se desenvolvem no tubo digestivo do intestino do mosquito e se diferenciam em uma forma chamada promastigota pró-cíclicas.[14-16] Depois disso, o protozoário invade as porções anteriores do estômago e desenvolvem uma forma flagelada chamada promastigota metacíclica que é capaz de infectar mamíferos durante o repasto sanguíneo.[16-18]

Após a inoculação pela picada do inseto, os neutrófilos são as primeiras células a serem recrutadas no local, seguido pelas células dendríticas e macrófagos. Estas células fagocitam a forma promastigota por mecanismos mediados por receptores e ligantes, entretanto apesar da ação de mecanismos de defesa, alguns parasitas conseguem sobreviver devido à indução da produção de células imunossupressoras como a citocina TGF-β que age inibindo a ativação de macrófagos.[19-23] A TGF-β

consegue suprir a produção de lL-12 que está relacionada com a diferenciação das células T em células Th_1, as quais são responsáveis pela secreção de citocinas como a IFN-y que atuam contra o parasita.[22,24] Assim, as promastigotas ficam alojadas em fagossomos. Nos macrófagos, os fagossomos se fusionam a lisossomos, formando um fagolisossomo chamado vacúolo parasitóforo.[7,25-28]

Dentro do vacúolo parasitófaro, as promastigotas se diferenciam em amastigotas e começam a se multiplicar até romperem a membrana da célula hospedeira.[7,28,29] Uma vez liberadas na corrente sanguínea, as amastigotas podem infectar novas células dendríticas, fibroblastos, bem como outros macrófagos.[28,29] O ciclo de transmissão se completa quando mosquitos não infectados ingerem sangue contendo fagócitos infectados[7] (Figura 1).

Figura 1: Ciclo de vida da *Leishmania* em mamíferos

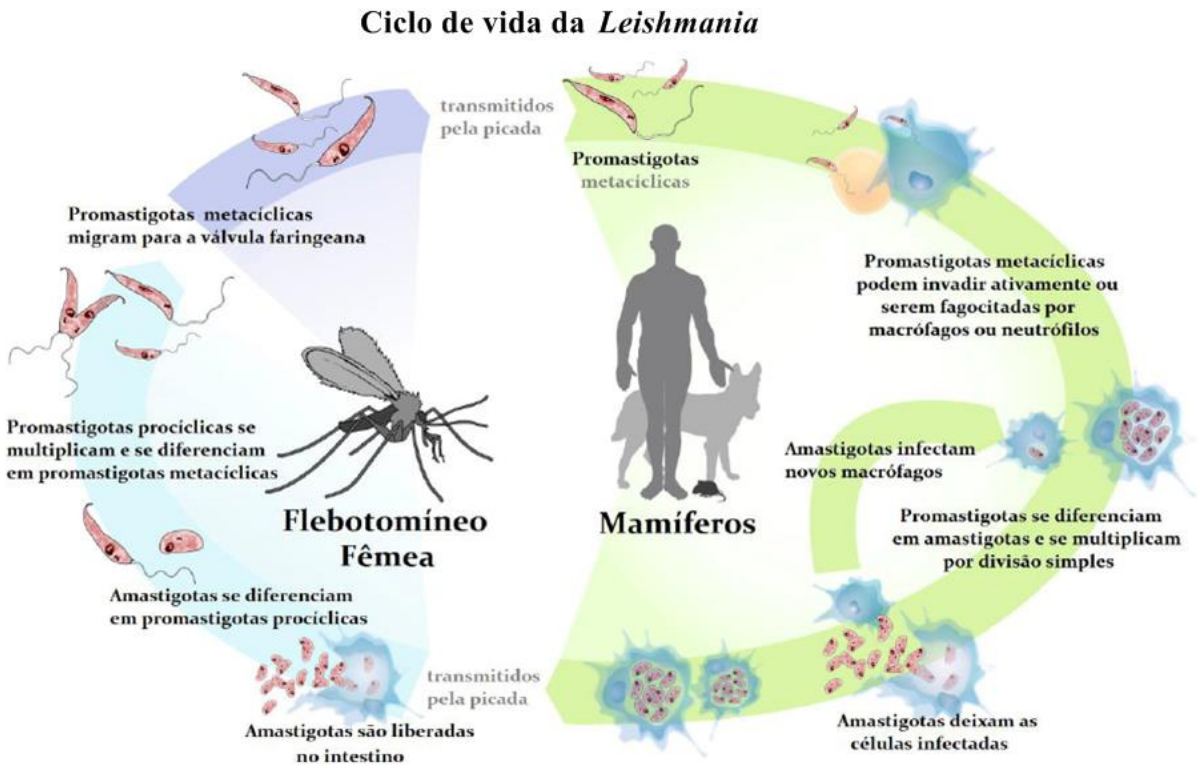

Fonte: adaptado de http://www.canalciencia.ibict.br/

1.4 TRATAMENTO

Os compostos antimoniais pentavalentes (Sb^{+5}) são considerados os fármacos de primeira linha para o tratamento da leishmaniose.[3] Encontram-se disponíveis duas formulações: Stibogluconato de sódio (Pentostan®) e o antimoniato-N-metil glucamina (Glucatime®).[3,30-32] No Brasil, apenas o segundo fármaco citado é atualmente distribuído pelo Ministério da Saúde.[3] Embora o mecanismo de ação do antimoniato-N-metil glucamina não esteja totalmente esclarecido, sabe-se que atua nas formas amastigotas do parasita, inibindo sua atividade glicolítica e a via oxidativa de ácidos graxos.[3,31] Devido ao surgimento de resistência primária do parasita a esses fármacos, principalmente em países como Sudão e Índia, o centro de Controle de doenças dos Estados Unidos da América e a OMS tem recomendado nos últimos anos doses superiores dos antimoniais.[3] Estes medicamentos têm como desvantagem o alto custo e baixa aderência ao tratamento devido à necessidade de administração em um ambiente hospitalar aliado a um tratamento prolongado (de 20 a 40 dias).[3,33,34] Além disso, estes fármacos podem causar diversos efeitos adversos e são contraindicados para gestantes e pacientes com insuficiência renal ou hepática.[3, 34]

Outro fármaco disponível atualmente é a anfotericina B, ela atua tanto nas formas promastigotas quanto amastigotas do parasita. Seu mecanismo de ação se dá através da ligação com ésteres (ergosterol e episterol) presentes na membrana plasmática do parasita.[3,35] É considerado o fármaco de primeira linha para gestantes e pacientes HIV-positivos e o de segunda linha mais utilizado quando o tratamento com os Sb^{+5} não apresentam resultados.[3,35,36] Além deste medicamento também possuir tratamento prolongando e necessidade de administração em ambiente hospitalar, ainda existe a necessidade de monitoramento eletrocardiográfico e laboratorial das enzimas hepáticas e função renal, devido aos efeitos colaterais que podem surgir, como a insuficiência renal e hepática e alterações cardíacas.[35,36] Recentemente, novas formulações de anfotericina B (anfotericina-B-lipossomal e anfotericina B-dispersão coloidal) tornaram-se disponíveis comercialmente.[3,37] A forma lipossomal é considerada menos tóxica, porém o uso em regiões onde a doença é endêmica é restringido devido a seu elevado custo. [3, 37, 38]

Em 2014, a agência reguladora norte-americana FDA (*Food and Drug Administration*) aprovou o medicamento Mitefosina. É o único medicamento que possui administração por via oral para tratar leishmaniose, ensaios demonstraram que ele é seguro e eficaz no tratamento da leishmaniose mucosa, LV e LC.[38] O medicamento mostrou resultados para o tratamento de LC causada por *L. panamensis, L. mexicana* e *L. guyanensis*, porém é ineficaz contra lesões causadas por *L. braziliensis*. [38] Apesar de este medicamento apresentar menos efeitos adversos comparado com os já utilizados, ele não pode ser administrado em gestantes. [29,39]

Outras alternativas para tratar a LC é a utilização de medicamentos tópicos associados com outros fármacos antimoniais, como a Imiquimoda e a Paromomicina, que vem demonstrando resultados positivos.[38, 39] Estudos mostraram que o uso tópico do fator estimulante de colônias de granulócitos e macrófagos (GM_CSF) leva a aceleração da cicatrização das lesões causadas pelo parasita.[40,41]

Neste contexo, é de grande necessidade o estudo de novos alvos moleculares e o desenvolvimento de fármacos para o tratamento da leishmaniose que apresentem alta especificidade e seletividade.

1.5 METABOLISMO DE PURINAS

O planejamento racional de fármacos normalmente é baseado em explorar as diferenças bioquímicas e fisiológicas entre o patógeno e o hospedeiro com a finalidade de encontrar potenciais alvos moleculares para a ação de novos inibidores.[42-45] O metabolismo de nucleotídeos de purinas se diferencia muito entre *Leishmania* e seu hospedeiro mamífero.[45] Os nucleotídeos são moléculas orgânicas que participam de vários processos bioquímicos essenciais para todos os organismos vivos. Eles são as unidades monoméricas do DNA e RNA; adenosina trifosfato (ATP) e guanosina trifosfato (GTP), quando hidrolisados, dirigem processos que requerem energia livre; ATP, adenosina difosfato (ADP) e adenosina monofosfato (AMP) atuam como reguladores de diversas rotas metabólicas; adenosina monofosfato cíclico (AMPc) e guanosina monofosfato cíclico (GMPc) medeiam a sinalização hormonal, e por fim NAD+, NADP+, FAD e coenzima A são coenzimas essenciais para uma grande variedade de reações enzimáticas.[46-49]

Em mamíferos, nucleotídeos de purinas podem ser obtidos através da via *de novo* ou rota de salvamento. A via *de novo* (Figura 2) inicia a partir de compostos simples para a síntese de nucleotídeos de purinas (aminoácidos, ribose-5-fosfato, CO_2, NH_3), onde a porção ribose fosfato dos nucleotídeos é obtida a partir do 5-fosforribosil-1-pirofosfato (PRPP) sintetizado a partir de ATP e 5-fosforribose, e termina após 11 reações enzimáticas dependentes de ATP com a síntese de inosina monofosfato (IMP). A IMP pode ser convertida em AMP ou guanosina monofosfato (GMP) através de duas vias representadas na figura 3.[48-51]

Figura 2: A via de biossíntese *de novo* de purinas em mamíferos.

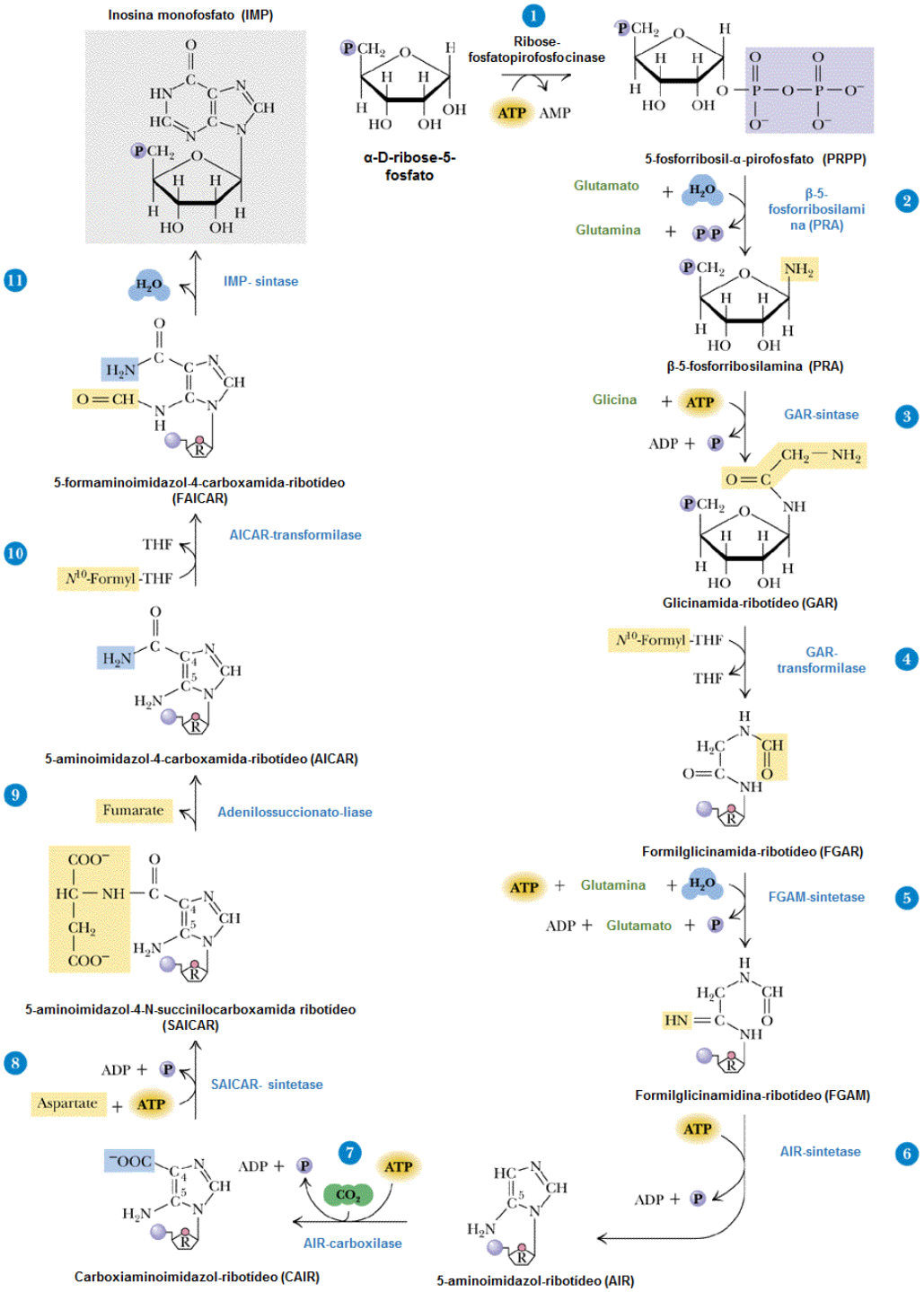

Fonte: Adaptado de Charles Grisham; Reginald H. Garrett, 2002.

Figura 3: Conversão de inosina monofosfato (IMP) em adenosina monofosfato (AMP) ou guanosina monofosfato (GMP) na rota de biossíntese de purinas.

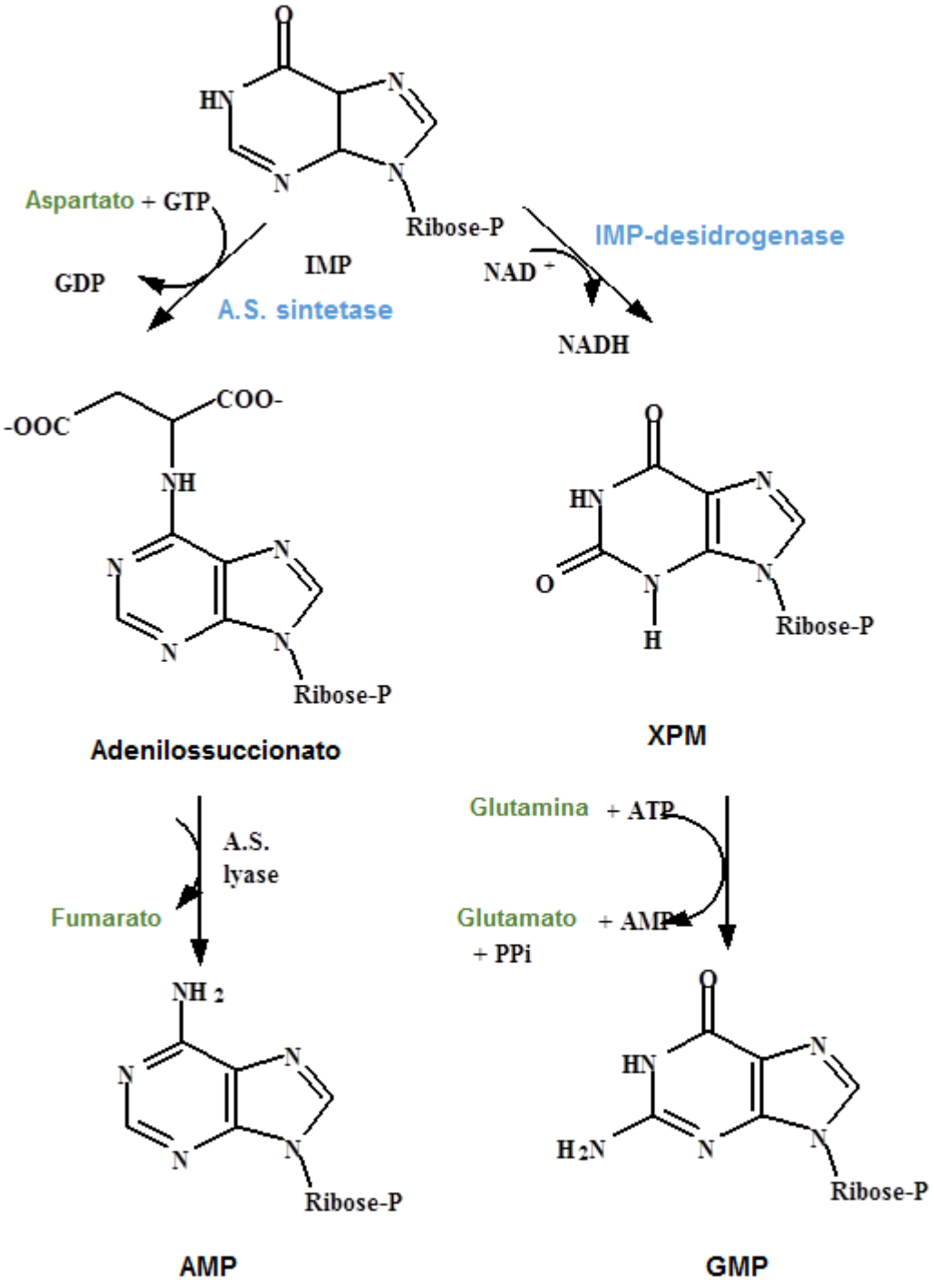

Fonte: Adaptado de http://themedicalbiochemistrypage.org/

Já a via de salvamento (figura 4) de purinas é considerada mais simples quando comparada com a biossíntese *de novo*. Nela, ocorre a recuperação de nucleotídeos pré-formados como adenina, guanina e hipoxantina resultantes da degradação de ácidos nucléicos ou de nucleotídeos livres, através da reação direta do PRPP com as purinas livres, que são convertidas em IMP, AMP e GMP pela ação de enzimas fosforibosiltransferases (PRTases) correspondentes.[50,51]

Figura 4: Via de salvamento de purinas em *Leishmania*

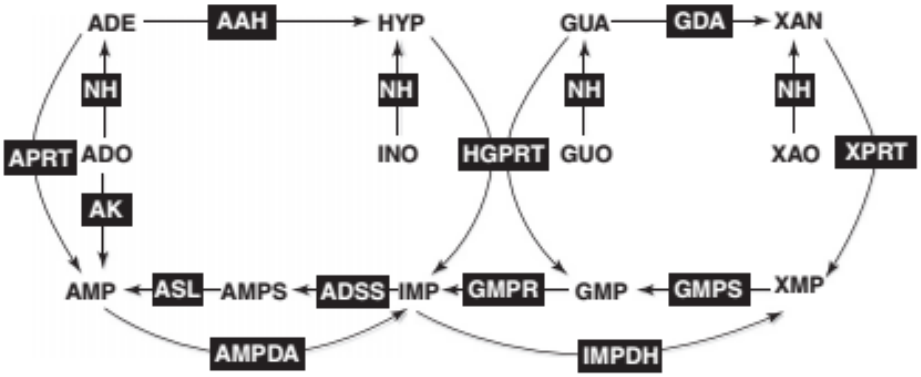

Figura 4: Via de salvamento em *Leishmania*. Abreviações: APRT, adenina fosforribosiltransferase, HGPRT, hipoxantina-guanina fosforribosiltransferase, XPRT, xantina fosforribosiltransferase, AK, adenosina quinase, AAH, adenina aminohidrolase, GDA, guanina deaminase, ADSS, adenilosuccinato sintetase, ASL, adenilosuccinato liase, AMPDA, adenosina monofosfato deaminase, IMPDH, inosina monofostafase desidrogenase, GMP, guanosina monofosfato sintetase, GMPR, guanosina monofosfato redutase, NH, nucleosídeo hidrolase, ADO, adenosina, INO, inosina, HYP, hipoxantina, GUO, guanosina, GUA, guanina, XAO, xantosina, XAN, xantina. Fonte: Jan M. Boitz *et al*. 2012.

Uma característica marcante de muitos protozoários, como *Trichomonas vaginalis*,[52] *Trypanosoma brucei*,[53] e *Crithidia fasciculata*,[54] incluindo espécies de *Leishmania tarentolae*,[55] *Leishmania mexicana*,[56] *Leishmania donovani* e *Leishmania braziliensis,* [57] é a falta da via de biossíntese *de novo* de nucleotídeos, o que os torna auxotróficos para purinas e dependentes da via de salvamento para a síntese de nucleotídeos.[48,58-60] Esses organismos possuem uma extensa via de salvamento de

nucleotídeos que lhes permite reutilizar purinas do hospedeiro, sendo capazes de incorporar nucleosídeos ou bases purínicas.[46-48,60] A obrigatoriedade do uso do salvamento de purinas pelo parasita oferece, portanto, uma grande quantidade de alvos moleculares potencias para o desenvolvimento de novos candidatos a fármacos.[60-62]

1.6 NUCLEOSÍDEOS HIDROLASES

As nucleosídeos hidrolases (NH) são enzimas que tem papel central na rota de salvamento de purinas, elas catalisam a hidrólise irreversível da ligação N-glicosídica de ribonucleosídeos formando α-D-Ribose e a base púrica livre corresponde (figura 5).[62-65] As NH já foram identificadas em muitos organismos como: bactérias,[66,67] insetos [68] e protozoários.[62,65,69-72] Entretanto nenhuma atividade de NH foi encontrada em mamíferos, uma vez que em eucariotos, a base purínica dos nucleosídeos é liberada pela reação de fosforilase catalizada pela enzima fosforilase de nucleosídeos de purinas (PNP).[63, 69]

Diversos estudos mostram diferentes especificidades de substrato entre as NH e por isso elas são classificadas em grupos conforme sua atividade catalítica:

-NH específica para inosina e uridina (IU-NH);[62, 65]

-NH específica para inosina, adenosina e guanosina (IAG-NH);[70,71]

-NH específica para inosina e guanosina (IG-NH).[72]

Entretanto, alguns estudos indicam que essa classificação é um pouco inadequada, pois um número crescente de NHs identificadas não se encaixam perfeitamente nas funções propostas por estes grupos.[60] NHs preferem substratos de purina, mas também catalizam reações envolvendo nucleosídeos de pirimidinas.[62,72-74]

Figura 5: Hidrólise de uridina e inosina pela nucleosídeo hidrolase (NH)

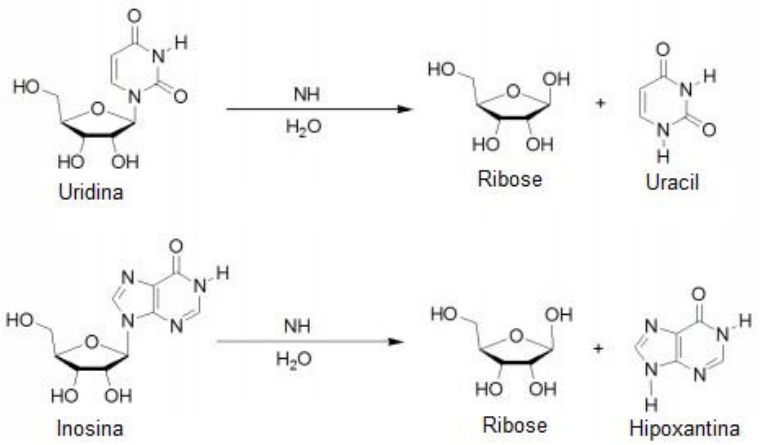

Fonte: Adaptado de Figueroa-Villar, José D.; Sales, Edijane M.

A hidrólise realizada pelas enzimas NHs é necessária para que os protozoários utilizem nucleosídeos de indivíduos infectados e os transformem em nucleobases para síntese de DNA. Como já mencionado anteriormente, uma das diferenças metabólicas entre os protozoários e os mamíferos é a ausência da via de biossíntese *de novo* de purinas, o que faz com que os parasistas dependam exclusivamente da reciclagem de nucleotídeos e nucleosídeos do hospedeiro para sobreviver.[71,65,69] Por esse motivo, a enzima NH de *Leishmania* pode ser um alvo molecular interessante para a obtenção de inibidores visando o tratamento da leishmaniose em pacientes infectados.

A IU-NH ganha destaque entre elas, pois além de ser a mais ambudante entre as hidrolases, é considerada uma enzima não específica que catalisa a hidrólise não só de inosina e uridina, mas também de adenosina, guanosina e citidina em alguns protozoários.[62,64,65,75] As propriedades cinéticas e as características estruturais das enzimas NHs de *Trypanosoma cruzi* [69], *Crithidia fasciulata* [75], *L. major* [65] e *L. donovani* [64] já foram descritas anteriormente. Além disso, muitos estudos permitiram o desenvolvimento de inibidores que se assemelham a propriedades geométricas e eletrônicas do estado de transição que já foram sintetizados e provaram ser poderosos inibidores competitivos [63,76,77]. Os iminoribitols 1-subistituentes são considerados ótimos inibidores para estas enzimas. Exemplos de inibidores como o 9-deazadenosina

(immucillin A) (Figure 6A) ou 4-amino-5-carbonilamino-3-pirrolil (immucillin ACAP) (Figure 6B) substituintes do iminoribitol, mostraram uma ótima inibição frente às NH de *C. falsiculata, T. brucei* e *L. major*.[65] Nos experimentos, estes inibidores competiram favoravelmente mesmo em grandes concentrações de substrato e pequenas de inibidor. Outro estudo recente, mostra efeitos positivos de outros derivados (Immucilin IA, IH e SMIH), os quais impediram a multiplicação *in vitro* das formas amastigotas e promastigotas de *L. infantum*, *L. chagasi* e *L. amazonenses*, e podem ser futuros candidatos contra a leishmaniose.[78]

Figure 6: Inibidores do estado de transição para nucleosídeos hidrolases (NH)

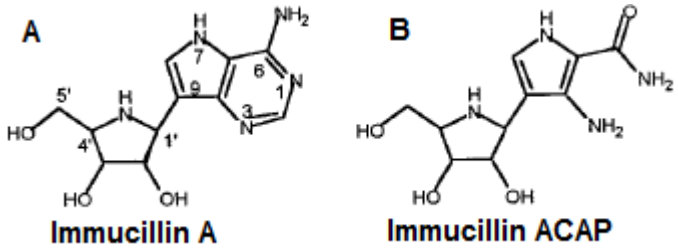

Fonte: Adaptado de Shi et al., 1999

Embora as NHs compartilhem um alto grau de similaridade de sequência entre estes protozoários, elas apresentaram propriedades cinéticas e estruturais diferentes. Nenhum estudo sobre estas características da enzima IU-NH *de L. braziliensis* (*Lb*IU-NH), principal agente etiológico de leishmaniose cutânea e mucocutânea no Brasil, foi publicado.

2. JUSTIFICATIVA

A leishmaniose é considerada uma das principais doenças endêmicas do mundo. Segundo a OMS aproximadamente 2 milhões de novos casos são registrados no mundo a cada ano e o Brasil está incluído entre os países com maior incidência da doença. As formas de leishmaniose cutânea e mucocutânea são as mais frequentes no país, e são causadas principalmente pela espécie *L. braziliensis*. Embora esta doença tenha tratamento, os medicamentos contra a leishmaniose apresentam muitos efeitos adversos e precisam ser administrados por tempo prologando em ambiente hospitalar, o que leva a não aderência do paciente ao tratamento. Neste cenário, o desenvolvimento de novos fármacos para o tratamento da leishmaniose é de extrema necessidade.

A rota de salvamento de purinas possui alvos atrativos para o desenvolvimento de novos fármacos, uma vez que ela é essencial para a viabilidade do parasita. Além disso, algumas enzimas envolvidas na via se diferenciam ou não estão presentes no hospedeiro mamífero. Assim, a melhor compreensão da via de salvamento de purinas pode revelar detalhes da biologia de *L. braziliensis* que podem contribuir para o desenvolvimento de novas estratégias para combater este parasita. A enzima *Lb*IU-NH pertence a rota de salvamento de purinas de *Leishmania* e não foi identificada em mamíferos. A caracterização bioquímica e estrutural da enzima *Lb*IU-NH é uma etapa importante na validação de um novo alvo molecular para o desenvolvimento racional de fármacos para leishmaniose.

3. OBJETIVOS

3.1 OBJETIVO GERAL

Caracterização enzimática e obtenção da estrutura cristalográfica da enzima inosina-uridina nucleosídeo hidrolase de *L. braziliensis.*

3.2 OBJETIVOS ESPECÍFICOS

1. Clonar o gene *iunH* de *L. braziliensis*, que codifica para enzima *Lb*IU-NH no vetor pET23a(+);
2. Expressar em *Escherichia coli* e purificar a proteína recombinante;
3. Identificar a identidade da proteína por espectrometria de massa;
4. Determinar o estado oligomérico em solução;
5. Determinar atividade enzimática, os parâmetros cinéticos em estado estacionário e os efeitos de pH;
6. Determinar a energia de ativação para obter parâmetros termodinâmicos de ativação;
7. Determinar os parâmetros termodinâmicos de ligação dos produtos;
8. Identificar possíveis efeitos isotópicos do solvente;
9. Determinar a estrutura trimendisional da proteína.

Capítulo 2

Artigo Científico

Artigo científico submetido ao periódico *Journal of Biochemical Chemistry* intitulado "Thermodynamics, Functional and Structural Characterization of Inosine-Uridine Nucleoside Hydrolase from *Leishmania braziliensis* "

MS ID#: JBC/2017/778027
Title: Thermodynamics, Functional and Structural Characterization of Inosine-Uridine Nucleoside Hydrolase from Leishmania braziliensis

Dear Dr. Basso:

We have received your manuscript entitled: Thermodynamics, Functional and Structural Characterization of Inosine-Uridine Nucleoside Hydrolase from Leishmania braziliensis

It has been given the number MS ID# JBC/2017/778027 and has been assigned to the following JBC Associate Editor who will manage the review process:

F. Peter Guengerich, Ph.D.
Deputy Editor
The Journal of Biological Chemistry
E-mail: ktrisler@asbmb.org

Manuscripts submitted under multiple authorship are reviewed on the assumption that all authors concur in the submission and that the final version of the manuscript has been seen and approved by all authors. Papers are published with the implicit understanding that you will pay all publication charges, as detailed here: www.jbc.org/site/misc/ifora.xhtml#PubCharges.

The Journal of Biological Chemistry: Instructions for Authors

www.jbc.org

Overview of submission and review process. The following is a brief overview of the submission and review process for JBC papers, along with links to the relevant ...

Thermodynamics, Functional and Structural Characterization of Inosine-Uridine Nucleoside Hydrolase from *Leishmania braziliensis*

Pedro Ferrari Dalberto[‡], Leonardo Kras Borges Martinelli[‡], Jose Fernando Ruggiero Bachega[§], Luis Fernando Saraiva Macedo Timmers[§], Antonio Frederico Michel Pinto[‡], Adilio da Silva Dadda[‡], Guilherme Oliveira Petersen[‡], Fernanda Teixeira Subtil[‡], Luiza Galina[‡], Anne Drumond Villela[‡], Kenia Pissinate[‡], Pablo Machado[‡], Cristiano Valim Bizarro[‡], Osmar Norberto de Souza[§], Edgar Marcelino de Carvalho Filho[¶], Luiz Augusto Basso[‡1], and Diogenes Santiago Santos[‡1]

From [‡]Centro de Pesquisas em Biologia Molecular e Funcional (CPBMF), [§]Laboratório de Bioinformática, Modelagem e Simulação de Biossistemas (LABIO), Pontifícia Universidade Católica do Rio Grande do Sul (PUCRS), Porto Alegre 90650-001, RS, Brazil, and [¶]Hospital Universitário Professor Edgard Santos, Universidade Federal da Bahia, Salvador 40110160, BA, Brazil

Running Title: *IU-NH from Leishmania braziliensis*

[1]To whom correspondence may be addressed: Luiz A. Basso (e-mail: luiz.basso@pucrs.br) or Diogenes S. Santos (e-mail: diogenes@pucrs.br), Centro de Pesquisas em Biologia Molecular e Funcional, Pontifícia Universidade Católica do Rio Grande do Sul, 92A building at TECNOPUC, 4592 Bento Gonçalves avenue, Porto Alegre, RS – Brazil 90650-001, Telephone: +55 (51) 3320-3629.

Keywords: Leishmania, enzyme catalysis, hydrolase, protozoan, IU-NH, purine salvage, *Leishmania braziliensis*, biochemical characterization, crystallography

ABSTRACT

Leishmaniasis is considered one of the main endemic diseases in the world, and Brazil is among the countries which has the highest incidence of cutaneous and mucocutaneous forms of leishmaniosis caused mainly by *Leishmania braziliensis*. Although treatment to this disease is available, the first-line drugs against leishmaniosis have several limitations: parenteral administration, long duration of treatment, and serious toxicities. One key metabolic characteristic of these parasites is the lack of *de novo* purine biosynthesis pathway, making them auxotrophic to purines. Accordingly, they rely solely on the purine salvage pathway for nucleotide synthesis. A better understanding of the purine salvage pathway can reveal details of the biology of *L. braziliensis* that could, in turn, be used to develop new strategies to combat this parasite. The inosine-uridine nucleoside hydrolase from *L. braziliensis* (*Lb*IU-NH) plays an important role in the salvage process and is an attractive drug target as there is no similar catalytic activity in mammals. Here, it is described cloning, heterologous protein expression, and a three-step purification protocol that yielded homogenous recombinant protein. Determination of *Lb*IU-NH steady-state kinetic constants for inosine, adenosine, cytidine and uridine are also reported. These data suggest that *Lb*IU-NH displays characteristics of a nonspecific hydrolase. Thermodynamic profile suggests that α-D-ribose can bind to free enzyme with favorable enthalpic (ΔH) and entropic (ΔS) contributions. Thermodynamic activation parameters (E_a, $\Delta G^{\#}$, $\Delta S^{\#}$, $\Delta H^{\#}$) for the *Lb*IU-NH-catalyzed chemical reaction, pre-steady-state kinetics, solvent kinetic isotope effects, and pH-rate profiles are also presented. In addition, the crystal structure of *Lb*IU-NH in complex with β-D-ribose and Ca^{2+} at 1.5 Å resolution is described.

INTRODUCTION

Trypanosomatidae family consists of protozoan parasites that can cause various diseases. Amongst its members, *Leishmania* is one of great importance, especially in Brazil, where the species *L. (V.) braziliensis*, *L. (L.) amazonensis* and *L. (L.) infant chagasi* have been identified.[1;2] These protozoans are flagellated parasites that can cause several dermatological and visceral manifestations in mammals, known as leishmaniosis. This disease is an antropozoonose with great veterinary and medical significance.[3;4] Its transmission is mediated by a female sand fly

of Phlebotominae subfamily of the genus *Lutzomyia*. The mosquito is responsible for transferring the amastigote form from one mammal to another. This protozoan goes through drastic physiological changes in its host, going from the extracellular promastigote form in the mosquito's intestine to the intracellular amastigote form macrophage's phagolysosomes of mammals.[4;5] Brazil is among the countries with the highest incidence of the cutaneous and mucocutaneous forms of leishmaniosis, which are present in almost every Brazilian state. Additionally, there are several reported cases of fatal visceral leishmaniosis.[6]

Although a treatment to this disease is available, the first-line drugs against leishmaniosis have several limitations regarding the administration route, which is usually parenteral, and the duration of treatment, that is at least three weeks.[7] Antimonial treatments require cautious medical attention because of side effects such as nausea, weakness and cardiotoxicity.[8] In addition, there have been reported cases of resistance, which led to the development of second-line drugs, pentamidine and amphotericin B. These new compounds, although effective against resistant organisms, are equally limited regarding their parenteral administration and severe side effects.[9] Even though there have been the development of new FDA approved drugs for leishmaniosis treatment (liposomal formulation of amphotericin B and miltefosine), these drugs are costly, difficult to administer, and poorly stable at high temperatures, typical of endemic regions.[10;11] Efforts to discover new anti-leishmanial agents are thus worth pursuing.

One key metabolic characteristic of these parasites is the lack of purine de novo biosynthesis pathway, making them auxotrophic to purines, and relying solely on the purine salvage pathway for nucleotide synthesis.[5;12;13;14] Nucleoside hydrolases are members of this pathway that irreversibly hydrolyze the *N*-glycosidic bond of ribonucleosides, forming α-D-ribose and the corresponding base.[15] Several nucleoside hydrolase isoenzymes have been studied and shown to have different substrate specificities. IU-nucleoside hydrolase is considered to be a nonspecific enzyme that catalyzes the hydrolysis of inosine and uridine.[16;17] More specifically, the IU-NH is a Ca^{2+}-dependent metalloenzyme that converts inosine to hypoxanthine and uridine to uracil.[14;18] Interestingly, no similar catalytic activity is present in mammals, which suggests that this enzyme has a specific role in the protozoan life cycle. Therefore, this offers an opportunity to develop inhibitors of protozoan nucleoside hydrolase enzyme activity.[19;20]

Several studies have reported the kinetic properties and structure of this enzyme in other tripanossomatidae organisms such as *Trypanosoma cruzi*,[21] *Crithidia fasciculata*,[20;22] *Leishmania major*[17] and *Leishmania donovani*.[5] Even though these enzymes share a high degree of sequence similarity, they show different kinetic and structural properties. In this work, we address the open questions regarding these characteristics for IU-NH from *L. braziliensis*, which is the main causative agent of leishmaniosis in Brazil.

Here, it is described cloning, heterologous protein expression, and purification of recombinant *L. braziliensis* IU-NH protein (*Lb*IU-NH). Steady-state kinetic constants for inosine, adenosine, cytidine and uridine substrates are presented. The thermodynamic parameters (ΔH, ΔS, and ΔG) for α-D-ribose binding to *Lb*IU-NH were determined by isothermal titration calorimetry (ITC). In addition, studies of pH-rate profiles, thermodynamic activation parameters (E_a, $\Delta G^{\#}$, $\Delta S^{\#}$, $\Delta H^{\#}$), solvent kinetic isotope effects and pre-steady-state kinetics were carried out to elucidate the chemical and catalytic mechanisms of *Lb*IU-NH-catalyzed chemical reaction. The crystal structure at 1.5 Å resolution of *Lb*IU-NH in complex with β-D-ribose and Ca^{2+} is also described.

RESULTS

Cloning, expression and purification

LbrM.18.1610 gene, synthesized by Biomatik®, was cloned into the pET23a(+) expression vector. Nucleotide sequence analysis of the gene confirmed both identity and integrity, showing that no mutations were introduced by cloning steps. Sodium dodecyl sulfate polyacrylamide gel electrophoresis (SDS-PAGE) analysis of *Escherichia coli* Rosetta (DE3) host cells with recombinant pET23a(+)::LbrM.18.1610 plasmid showed expression in the soluble fraction of a recombinant protein with an apparent subunit molecular mass of ~34 kDa. This result is in

agreement with the expected molecular mass of *Lb*IU-NH (34,340 Da). A three-step purification protocol (anionic exchange followed by hydrophobic interaction and size exclusion) was developed that yielded 10 mg of homogenous recombinant *Lb*IU-NH protein per gram of wet cell paste (frozen cells).

_Lb_IU-NH identification by mass spectrometry

The protein band in SDS-PAGE of approximately 34 kDa was excised, submitted to trypsin digestion protocol and the peptides analyzed by LC-MS/MS. From the analysis in duplicate, *Lb*IU-NH (A4H9Q9) identity was confirmed, with the identification of 43 unique peptides, 400 spectral counts and sequence coverage of 74.8 %.

Oligomeric state determination

A value of 136,019 for the apparent molecular mass of homogeneous recombinant *Lb*IU-NH was estimated by gel filtration chromatography, fitting the elution volume of the single peak to Eq. 1 (Fig. S1, Supplemental Data). The gel filtration result suggests that *Lb*IU-NH is a tetramer in solution.

Steady-state kinetic parameters

Saturation curves for specific activity of *Lb*IU-NH against increasing concentration of inosine (Fig. 1A), adenosine (Fig. 1B), cytidine (Fig. 1C), uridine (Fig. 1D), and guanosine (Fig. 1E) were evaluated. Steady-state kinetic parameters are given in Table 1. The hyperbolic saturation curve data for inosine were fitted to the Michaelis-Menten equation (Eq. 2). The results for adenosine, cytidine and uridine were first fitted to a linear equation to obtain initial velocity values, which were in turn plotted as a function of increasing substrate concentrations. Data for adenosine and cytidine were fitted to Michaelis-Menten equation (Eq. 2), and the sigmoidal data for uridine were fitted to Eq. 4. Owing to limited solubility, the steady-state parameters for guanosine could not be determined as no saturation was achieved. Nevertheless, a linear increase in activity could be detected (Fig. 1E) suggesting that the initial phase of the hyperbolic curve was being observed, which only allows an estimate for k_{cat}/K_m to be obtained for guanosine (Table 1).

Isothermal titration calorimetry

Isothermal titration calorimetry (ITC) allows monitoring of binding reactions with direct measurements of heat taken or released upon binding of a ligand, providing the binding enthalpy of the process (ΔH), an estimate for the stoichiometry of the interaction (n), and the equilibrium constant (K_a). These results allow the dissociation constant (K_d), Gibbs free energy (ΔG) and the entropy (ΔS) to be calculated. ITC binding assays showed that α-D-ribose can bind to free *Lb*IU-NH enzyme (Fig. 2), yielding the following thermodynamic parameters: ΔH = -1.3 ± 0.4 kcal mol^{-1}, ΔG = -5.0 ± 1.3 kcal mol^{-1} and ΔS = 12.5 ± 3.4 cal mol^{-1} K^{-1}, n = 1.6 ± 0.4 sites, and K_d = 192 ± 48 μM. No binding of free bases (hypoxanthine, and uracil) could be detected by ITC.

Energy of activation

The energy of activation for the enzyme catalyzed chemical reaction was assessed by measuring the dependence of k_{cat} on temperature for inosine. The linearity of the Arrhenius plot (Fig 3) suggests that there is no change of the rate-limiting step over the temperature range utilized in the experiment. Thermodynamic activation parameters for *Lb*IU-NH-catalyzed chemical reaction were derived from data fitting to Eqs. 7-10, yielding the following values E_a = 3.8 ± 0.1 kcal mol^{-1}, $\Delta H^{\#}$ = 3.3 ± 0.2 kcal mol^{-1}, $\Delta S^{\#}$ = -42.75 ± 1.3 cal mol^{-1} K^{-1}, and $\Delta G^{\#}$ = 16.1 ± 0.02 kcal mol^{-1}.

Solvent kinetic isotope effects (SKIE) and proton inventory

Solvent kinetic deuterium isotope effects were determined to evaluate the contribution, if any, of proton transfer from solvent to a rate-limiting step in the *Lb*IU-NH-catalyzed chemical reaction. Data fitting to Eq. 12 yielded the following SKIE values: $^{D2O}V_{inosine}$ = 1.4 ± 0.1 and $^{D2O}V/K_{inosine}$ = 1.2 ± 0.1 (Fig. 4).

pH-rate profiles

The pH dependence of k_{cat} and k_{cat}/K_M for inosine was determined to probe acid-base catalysis and to evaluate the apparent acid dissociation constant for ionizing groups involved in the mode of action of *Lb*IU-NH. The bell-shaped pH-rate data for k_{cat} (Fig. 5A) were fitted to

Eq. 13, yielding apparent pK_a and pK_b values of, respectively, 5.2 ± 1.1 and 7.9 ± 1.9. The data of pH-rate profile for $k_{cat}/K_{inosine}$ were fitted to Eq. 14, yielding a value of 5.7 ± 0.5 for pK_a (Fig. 5B).

Pre-steady-state kinetics

Stopped-flow measurements of product formation were carried out to assess whether or not product release contributes to the rate limiting step. The pre-steady-state time course showed a linear decay (Fig. 6), and the data were thus fitted to Eq. 15, yielding a value of 0.0208 (± 0.0002) s^{-1} for the apparent first-order rate constant of product formation (k) and 2.3049 (± 0.0001) for A_0. The value of k corresponds to a catalytic rate constant value of 11.3 s^{-1}.

Crystal structure determination

Crystals of *Lb*IU-NH were obtained in orthorhombic space group (I222) and diffracted to a minimum d-spacing of 1.53 Å. The content of the asymmetric unity was determined by Matthews Coefficient ($C_{matthews}$ = 2.32), which corresponds to one monomer and solvent content of 47%. The initial electron density maps ($2F_o$-F_c and F_o-F_c) clearly showed evidence of a metal ion at the expected position as well as the presence of a β-D-ribose in the active site, confirming the correct phase attribution by molecular replacement. The refined model consists of one polypeptide chain, one calcium ion, one molecule of β-D-ribose and 278 water molecules (Table 2 shows data collection and refinement statistics). The electron density map ($2F_o$-F_c) is continuous for the main chain. The biological unity is sitting on spatial position so that the biological tetramer is generated from the symmetry operations of the space group I222.

DISCUSSION

Initial velocity and substrate specificity

The initial velocity experiments were carried out to determine the steady-state kinetic constants and substrate specificity (inosine, adenosine, cytidine, uridine and guanosine) of tetrameric *Lb*IU-NH. Steady-state kinetics results showed that K_M value for inosine (Table 1) was similar to other leishmania species such as *L. major* (K_M = 445 ± 209 μM) and *L. donovani* (K_M 329 ± 143 μM)[5;17] as expected due the sequence similarity among the species. However, uridine substrate was fitted to the Hill Equation due to its sigmoidal profile suggesting positive homotropic cooperativity for this substrate, with a Hill coefficient (n) value of 3.0. To the best of our knowledge, the sigmoidal profile has never been reported for NH enzymes of parasitic protozoa. However the nucleoside hydrolase from *Mycobacterium tuberculosis* has been shown to display positive cooperativity for inosine and adenosine.[23] Interestingly, the *Lb*IU-NH k_{cat} value for inosine is 10.6-fold lower as compared to *L. major* (119 s^{-1}),[17] and similar to *L. donovani* (7.6 s^{-1}).[5] The *Lb*IU-NH k_{cat} value for uridine substrate is lower than both *L. major* (32 s^{-1})[17] and *L. donovani*, (9.5 s^{-1}).[5]

Even though recombinant *Lb*IU-NH catalyzed the hydrolysis of purine and pyrimidine nucleosides, fairly low activity were observed for adenosine, cytidine and guanosine (Table 1). These results indicate that *L. braziliensis* has apparently evolved to preferentially catalyze hydrolysis of inosine and, to a lesser extent, uridine. Hypoxanthine is considered to be the major precursor for purine salvage in *L. braziliensis*. The *Lb*IU-NH enzyme displays two of three features that characterize the *L. major* enzyme as a nonspecific hydrolase, which are the recognition of inosine and uridine as the favorable substrates and activity with all naturally occurring purine and pyrimidine nucleosides (adenosine, guanosine and cytidine).[17] However, the apparent second-order rate constant values of *Lb*IU-NH for the latter substrates are considerably lower than *L. major* enzyme values.[17] It is not known yet whether *Lb*IU-NH catalyzes hydrolysis of *p*-nitrophenyl *β*-D-ribofuranoside, which is the third characteristic for all nonspecific hydrolases.[17] *Trypanosoma vivax* nucleoside hydrolase shows preference for inosine, adenosine and guanosine (IAG-NH) as suggested by the apparent second-order constant values, k_{cat}/K_M.[24] Although the *T. vivax* IAG-NH k_{cat} value (5.19 s^{-1}) for inosine is similar to *Lb*IU-NH k_{cat} one (11.2 s^{-1}), the overall dissociation constant (K_M) is 96-fold lower for *T. vivax* IAG-NH as compared to *Lb*IU-NH, resulting in a significant lower k_{cat}/K_M value for the latter enzyme. For adenosine, the k_{cat}/K_M value is approximately 2,600-fold larger for *T. vivax* IAG-NH[24] than for *Lb*IU-NH (Table 1). Owing to solubility issues of guanosine, only k_{cat}/K_M could

be estimated (Table 1), suggesting a value approximately 10,500-fold lower than for *T. vivax* IAG-NH enzyme.[24] The *Lb*IU-NH k_{cat} value for uridine (Table 1) is 200-fold larger than *T. vivax* IAG-NH.[24] However, *Lb*IU-NH displayed positive cooperativity for uridine with a Hill coefficient (*n*) value of 3.0, whereas *T. vivax* IAG-NH displayed Michaelis-Menten saturation curve for this substrate.[24] Although the overall dissociation constant values for cytidine are fairly similar for both enzymes, the *T. vivax* IAG-NH k_{cat} value[24] is at least 5-fold larger than *Lb*IU-NH. The steady-state kinetic data suggest that *Lb*IU-NH is a non-specific hydrolase, catalyzing the hydrolysis of naturally occurring purine and pyrimidine nucleosides. However, a preference for inosine is observed (Table 1).

Thermodynamic parameters and order of release of products

The binding of α-D-ribose to *Lb*IU-NH detected by ITC measurements showed that binary complex formation is an exothermic process as heat was released to the system (Fig. 2). No heat changes were detected for hypoxanthine and uracil binding to *Lb*IU-NH (data not shown), suggesting that these ligands cannot bind to free enzyme. Binding of adenine, guanine and cytosine could not be evaluated due to low solubility of these ligands in aqueous solutions. ITC data for α-D-ribose were best fitted to single set of sites model yielding an *n* (stoichiometry) value of 1.6 site per monomer of *Lb*IU-NH, indicating that one molecule of α-D-ribose binds to each enzyme active site with equal affinity. The thermodynamic profile suggests that α-D-ribose binding is a spontaneous process (ΔG = -5.0 kcal mol^{-1}) with favorable enthalpic (-1.3 kcal mol^{-1}) and entropic (12.5 cal mol^{-1} K^{-1}) contributions. The negative enthalpy can arise from favorable redistribution of the network of interactions (hydrogen bonds and/or van der Waals) between the reacting species (including solvent).[25] Hydrophobic interactions are related to the relative degrees of disorder in the free and bound system and thus these interactions are reflected in the entropy change. The release of water molecules from the reacting species to bulk solvent usually results in favorable positive entropic contribution.[25] The favorable enthalpic and entropic contributions resulted in a favorable negative ΔG value with no enthalpy-entropy compensation phenomenon for α-D-ribose binding to *Lb*IU-NH.

The ITC data indicate that the free base is the first product to be released followed by α-D-ribose dissociation to yield free *Lb*IU-NH enzyme for the next round of catalysis. Product inhibition studies for *C. fasciculata* nucleoside hydrolase have revealed a rapid-equilibrium random mechanism, in which both base (hypoxanthine) and α-D-ribose can bind to free enzyme.[16] However the dissociation constant value for α-D-ribose (700 μM) is approximately 10-fold lower than for hypoxanthine (6.2 mM).[16] The ITC data analysis for α-D-ribose binding to *Lb*IU-NH yielded a value of 192 μM, which is lower than for *C. fasciculata* nucleoside hydrolase,[16] and lower than for *M. tuberculosis* nucleoside hydrolase (10 mM).[23] As no heat change could be detected upon binding of hypoxanthine (5 mM) to *Lb*IU-NH, there appears to be no binding of this base to free enzyme. Product inhibition studies for *C. fasciculata* nucleoside hydrolase indicate weak hypoxanthine affinity for free enzyme.[16] Owing to limited solubility, larger concentrations of hypoxanthine could no be employed in the ITC experiments here described.

Energy of activation

The E_a value of 3.8 kcal mol^{-1} for inosine represents the minimum amount of energy necessary to initiate the *Lb*IU-NH-catalyzed chemical reaction. The linearity of the Arrhenius plot (Fig. 3) indicates that there is no change in the rate-limiting step over the temperature range employed (15 - 35 ºC). The values of free activation energy ($\Delta G^{\#}$) represent the energy barrier required for reactions to occur. The $\Delta G^{\#}$ values can also be regarded as the variation of the Gibbs energy between the enzyme:substrate(s) activated complex and reactants (enzyme and substrates) in the ground state. The negative value for the entropy of activation ($\Delta S^{\#}$ = -42.75 cal mol^{-1} K^{-1}) suggests that there is loss of degrees of freedom on going from the ground state to activated state. The enthalpy of activation ($\Delta H^{\#}$ = 3.3 kcal mol^{-1}) is related to the ease of bond breaking and making in the generation of the activated complex (transition-state complex) from reactants in the ground state. The lower $\Delta H^{\#}$ value,

the faster the rate. The enthalpy of activation for *Lb*IU-NH ($\Delta H^{\#}$ = 3.3 kcal mol^{-1}) suggests that more interatomic interactions (hydrogen bonds and/or van der Waals) are formed in the transition-state complex as compared to reactants in the ground state in bulk solvent.

Solvent kinetic isotope effects (SKIE) and proton inventory

Measurements of solvent kinetic isotope effects were carried out to assess the contribution of solvent proton transfer(s) to a step in the *Lb*IU-NH-catalyzed chemical reaction (Fig. 4). Solvent isotope effects on *V* are related to solvent-exchangeable protons being transferred during events following the ternary complex formation capable of undergoing catalysis (fully loaded enzyme), which include the chemical steps, possible enzyme conformational changes and product release (leading to regeneration of free enzyme). Solvent isotope effects on *V/K* arise from solvent-exchangeable protons being transferred during steps in the reaction mechanism from the binding of substrates to the first irreversible step, usually considered the release of the first product.[26] The value of 1.4 ± 0.1 for the solvent kinetic deuterium isotope effect on *V* indicates that solvent proton transfer partially limits hydrolysis of inosine in a step that occurs after substrate binding. The value of 1.2 ± 0.1 for the solvent kinetic deuterium isotope effect on *V/K* indicates a modest, if any, contribution to proton transfer step(s) between the free enzyme and substrate up to the first irreversible step. Similar solvent kinetic isotope effects were observed for *C. fasciculata* nucleoside hydrolase: 1.3 for *V* and 0.99 for *V/K*.[22] To assess the number of protons transferred during the solvent isotope-sensitive step, a proton inventory experiment was carried out. A linear relationship between *V* and the mole fraction of D_2O was obtained for *Lb*IU-NH (Fig. 4 - inset), suggesting that a single proton is transferred in the step that exhibits the solvent isotope effect. The mode of action of nonspecific nucleoside hydrolases involves a transition state with advanced cleavage of the N9-C1' ribosidic bond (0.22 bond order remaining), and attacking water nucleophile lagging behind N-ribosidic bond breaking with approximately 0.03 bond order from the attacking oxygen to C1', leaving the pentose as an oxocarbenium cation with C1' rehybridized nearly completely to sp^2.[17,19] The hypoxanthine leaving group is protonated at N7 prior to reaching the transition state, creating a neutral, planar and hydrophobic leaving group.[17,19] The ribooxocarbenium ion is assisted by conformational distortion of the sugar using protein contacts and a catalytic site Ca^{2+} to permit both the ring oxygen and the unshared electrons of 5'-hydroxymethyl oxygen to participate in the cleavage of the sugar-base bond. Solvent isotope effects are global and isotope exchange can occur at several protic positions of the enzyme. Accordingly, assigning the solvent isotope effects to a particular chemical step is not straightforward. Initial rate conditions for nucleoside hydrolases imply that cleavage of the ribosidic bond must be considered the first irreversible step.[22] It has thus been proposed that proton transfer is not a major part of the transition state, with the proton transfer having been completed prior to transition-state formation.[22] However, it is tempting to suggest that enzyme-activated water molecule may account for the, albeit modest, SKIE results for *Lb*IU-NH.

pH-rate profiles

The bell-shaped pH-rate profile for k_{cat} suggests participation of an ionizing group with apparent pK_a value of 5.2 that must be unprotonated and another group with pK_b value of 7.9 that must be protonated for catalysis to occur (Fig. 5A). The imidazole side chain of His240 residue is a plausible candidate for the group with pK_b value of 7.9, which is likely involved in protonation of hypoxanthine leaving group. The carboxyl group of Asp241 may be the unprotonated group involved in stabilization of the developing charge on the ribosyl oxocarbenium ion. Alternatively, the carboxyl groups of Asp241 or Asp10 may be involved in proton abstraction of an enzyme-bound water molecule for nucleophilic attack on C1' of nucleosides. The Ca^{2+} ion may lower the pK_a of this water molecule prior to proton transfer to the carboxyl group of Asp241 or Asp10. The His240 amino acid is conserved in *L. braziliensis* and its analogous has been proposed to be involved in leaving group activation of nucleoside hydrolases from *C. fasciculata* and *L. major*.[17;27] It has been shown that the His241Ala *C. fasciculata* IU-NH mutant showed a 2100-fold decrease in k_{cat} for inosine whereas there was a

2.8-fold increase in k_{cat} with *p*-nitrophenyl β-D-ribofuranoside.[27] These results showed that His241 of *C. fasciculata* IU-NH (His240 of *Lb*IU-NH) is the proton donor for leaving group activation as the *p*-nitrophenyl β-D-ribofuranoside substrate requires no stabilization of the nitrophenylate ion as leaving group.[27] The carboxylate group of Asp10 of *T. vivax* IAG-NH is involved in proton abstraction from a water molecule, while Asp40 donates a proton to N9 of the purine ring.[24] However, this mechanism for leaving group activation cannot be extended to *Lb*IU-NH because the equivalent amino acid at this position is an asparagine residue (Asn39), as found for *C. fasciculata* and *L. major* IU-NHs (Fig. S3, Supplemental Data).

The pH-rate data for $k_{cat}/K_{Inosine}$ (Fig. 5B) indicates that the deprotonation of a group with pK_a of 5.7 is required for inosine binding. Four aspartic acid residues were found to interact with the α-D-ribose moiety of nucleosides in the crystal structure of *C. fasciculata* IU-NH.[20] These residues are conserved in *Lb*IU-NH. The residues Asp10, Asp15, Asp241 and Thr126 are involved in interactions with Ca^{2+} ion in *Lb*IU-NH crystal structure (see below). The mechanistic role of Ca^{2+} is to orient substrate in the active site and to position the solvent for attack at C1' following the formation of the ribooxocarbenium ion.[28] If any of these residues is in the protonated form, they will not be able to interact with Ca^{2+}, precluding the orientation of the substrate and therefore abolishing substrate binding. Nevertheless, site-directed mutagenesis efforts will have to be pursued to ascertain whether or not His240 and Asp241 (or Asp10) play any role in catalysis, and which aspartate (Asp10, Asp15, Asp241) plays a role in substrate binding.

Pre-steady kinetics

There appears to be no burst of product formation (Fig. 6) at large subunit concentrations of *Lb*IU-NH (10 μM) and fixed-saturating concentration of inosine (2.0 mM). The value of 0.0208 for *k* ($\Delta A_{280nm}/t$) corresponds to a catalytic rate constant value of 11.3 s^{-1}, which is in good agreement with the results for steady-state kinetics (Table 1, 11.2 s^{-1}). Apparently, no signal was lost in the dead time of the equipment (1.37 ms). It was puzzling that the absorbance values for assay mixtures containing *Lb*IU-NH and inosine were larger than the values for the control experiment (Fig. 6), suggesting a hyperchromic effect. As NHs expel water molecules en route to product formation, the dielectric constant of the enzyme's active site is likely lower (polarity characteristic of an organic solvent). Estimates for the molar absorptivity values at 280 nm (ε_{280}) for inosine in solvents with different dielectric constants (D) were evaluated (Fig. S2, Supplemental Data). The values for ε_{280} were: 1.7 (± 0.3) x 10^3 M^{-1} cm^{-1} for Tris HCl 50mM (D_{water} = 78.74), 2.4 (± 0.1) x 10^3 M^{-1} cm^{-1} for MeOH (D_{MeOH} = 32.6) and 3.7 (± 0.1) x 10^3 M^{-1} cm^{-1} for DMSO (D_{DMSO} = 49).The dielectric constant values are: 78.74 for water, 49 for DMSO, and 32.6 for methanol. It is thus likely that the larger ε_{280} for the solution containing enzyme and inosine can account for the stopped-flow results. For electrostatic catalysis a reduction in the dielectric constant would result in an increase in the force between two charged molecules. Interestingly, charged molecules are present in the mode of action of nonspecific nucleoside hydrolases.[17,19] An alternative possibility is the difference of ε_{280} for the keto (lower value for the 6-keto) and the enol forms of inosine.[29]

Crystal structure determination

The overall structure is similar to those reported for *L. major* IU-NH (*Lm*IU-NH, PDB ID 1EZR),[17] *C. fasciculata* (*Cf*IU-NH, PDB ID 1MAS),[20] and *Escherichia coli* (*Ec*IU-NH, PDB ID 1Q8F).[30] The structure consists of one domain chain containing all the structural elements of these homologous enzymes (Fig. 7A). As observed for *Ec*IU-NH, the *Lb*IU-NH structure shows *cis*-bonds between residues Pro11-Gly12 and Tyr280-Pro281. All charged/polar residues in the active site are conserved (Fig. S3, Supplemental Data). The calcium ion is anchored by residues Asp10, Asp15, Asp241 and Thr126, forming a binding site.[31;32] The metal ion has eight coordination sites, five from the protein, in which Asp15 is involved in two interactions, two from the β-D-ribose molecule, and one water molecule (Fig. 7B). The β-D-ribose binding site is comprised of twelve residues, in which nine are involved in hydrogen bonds (Asp14, Asp15, Asn39, His82, Thr126, Asn160, Glu166, Asn168, and Asp241) and three

(Met152, Phe167, and His240) are making hydrophobic contacts. Regarding the conformational changes upon ligand binding, the loop between β3-α3 (Fig. S4, Supplemental Data) is found in a closed form, which allows the residue His82 to maintain contact to the β-D-ribose. This loop is also found in a closed form in the crystal structures of other holo nucleoside hydrolases.[18;30;33] An sp^2-hybridized C1' predicts a ribose with C3'-*exo* conformation (below the plane of the ring), whereas the C3'-*endo* puckering (above the plane of the ring) is favored for free inosine.[28] The β-D-ribose residue adopts a C2'-*endo* conformation similar to *E. coli* pyrimidine nucleoside hydrolase (PDB ID 1YOE; to be published), and in contrast to structures in complex with nucleosides that show the ribose having O4'-*endo* conformation.[24] As described in the EXPERIMENTAL PROCEDURES section, the crystallization solution contained D-(-)-ribose to take advantage of mutarotation of linear pentose. The *Lb*IU-NH crystal structure provides a snapshot of interactions between enzyme and a moiety of nucleoside substrates.

The surface contacts of the quaternary structure are very similar when compared to others IU-NHs, the dimer A-B interface is formed by mostly hydrophobic interactions involving helices α4, α7, the loop connecting β3-α3 and the loop connecting β9-β10 (contact area: 846.2 $Å^2$). The interface A-C is formed by interactions involving the loop connecting β5-α6 and the sheet formed by β9-β10 (contact area: 1068.8 $Å^2$). Interestingly, the *Lb*IU-NH structure shows an intermolecular disulfide bond between the interface of subunits A-D (and B-C), which has not been reported for other known structures of IU-NHs (Fig. 7C). The link occurs between the Cys157 and its symmetrical at the neighbor subunit, and the bond occurs coincidently with one 2-fold axis of the space group I222.

EXPERIMENTAL PROCEDURES

Cloning and protein expression

The *Lb*IU-NH coding gene LbrM.18.1610 was synthetized by Biomatik® and was cloned into the pET23a(+) expression vector using the *Nde*I and *Hind*III restriction enzymes. To confirm the product's identity and integrity as well as to ensure that no mutations were introduced in the cloned fragment, automatic DNA sequencing of LbrM.18.1610 gene was carried out.

The recombinant plasmid pET23a(+)::LbrM.18.1610 was transformed into *E. coli* Rosetta (DE3) electrocompetent host cells by electroporation and were grown on Luria-Bertani (LB) agar plates containing 50 μg mL^{-1} ampicillin and 34 μg mL^{-1} chloramphenicol. A single colony was cultivated overnight in 50 mL of LB at 180 rpm and 37°C. Nine milliliters of the culture were inoculated into 500 mL of LB medium with the same concentrations of antibiotics, and grown at 37°C and 180 rpm until an OD_{600} of 0.4, and grown further for 12 h at 30 °C with no IPTG induction. Cells were harvested by centrifugation at 8,000 × *g* for 30 min at 4°C and stored at -20°C.

Protein purification

Approximately 3 g of frozen cells were resuspended in 30 mL of 50 mM Tris HCl pH 7.5 (buffer A) containing 0.2 mg mL^{-1} of lysozyme (Sigma–Aldrich) and gently stirred for 30 min. Cells were disrupted by sonication (10 pulses of 10 s each at 60 % amplitude) and centrifuged at 48,000 × *g* for 30 min. To the supernatant was added 1% (v/v) streptomycin sulfate and gently stirred for 30 min. The solution was centrifuged at 48,000 × g for 30 min. The supernatant was dialyzed two times against 2 L of buffer A using a dialysis tubing with a molecular weight exclusion limit of 12,000-14,000 Da. This sample was centrifuged at 48,000 × *g* for 30 min and the debris-free supernatant was loaded on a Hiprep Q-Sepharose Fast Flow anion exchange column (GE Healthcare) pre-equilibrated with buffer A. The column was washed with 3 column volumes (CV) of the same buffer, and adsorbed proteins were eluted with a linear gradient (0-100 %) of 20 CV of 50 mM Tris HCl pH 7.5 containing 200 mM NaCl (buffer B) at 1 mL min^{-1} flow rate. Fractions containing the target protein were pooled and ammonium sulfate was added to a final concentration of 1 M, clarified by centrifugation at 48,000 × *g* for 30 min, and the resulting supernatant was loaded on a Hiprep Butyl Sepharose High Performance aliphatic hydrophobic column (GE Healthcare) pre-equilibrated with 50 mM Tris HCl pH 7.5 containing 1 M $(NH_4)_2SO_4$ (buffer C). This

hydrophobic column was washed with 10 CVs of buffer C and the adsorbed material eluted with 20 CVs of a linear gradient (0-100 %) of buffer A at 1 mL min^{-1} flow rate. The fractions containing the *Lb*IU-NH were pooled, concentrated down to 8 mL using an Amicon ultrafiltration cell (molecular weight cutoff of 10,000 Da), and loaded on a HiLoad Superdex 200 25/60 size exclusion column (GE Healthcare), which was previously equilibrated with buffer A. Proteins were isocratically eluted with 1 CV of buffer A at a flow rate of 0.3 mL min^{-1}. FPLC was performed in an AKTA system (GE Healthcare) and all purification steps were carried out at 4 °C and sample elution monitored by UV detection at 215, 254 and 280 nm simultaneously. Protein concentration was determined by the method of BCA using bovine serum albumin as standard (Thermo Scientific Pierce™ BCA protein Assay Kit). *Lb*IU-NH recombinant protein fractions were analyzed by SDS-PAGE.

_Lb_IU-NH identification by mass spectrometry

In-gel digestion was performed according to Shevchenko.[34] Tryptic digest of *Lb*IU-NH was separated on a in-house made 20 cm reversed phase column (5 µm ODSAQ C18, Yamamura Chemical Lab, Japan) using a nanoUPLC (nanoLC Ultra 1D plus, Eksigent, USA) and eluted directly to a nanospray ion source connected to a hybrid mass spectrometer (LTQ-XL and LTQ Orbitrap Discovery, Thermo, USA). The flow rate was set to 300 nL min^{-1} in a 120-minute reversed phase gradient. The mass spectrometer was operated in a data-dependent mode, with full MS1 scan collected in the Orbitrap, with m/z range of 400-1600 at 30,000 resolution. The eight most abundant ions per scan were selected to CID MS2 in the ion trap. Mass spectra were analyzed using PatternLab platform.[35] MS2 spectra were searched with COMET[36] using a non-redundant database containing forward and reverse *E. coli* DH10B reference proteome and the sequence of *Lb*IU-NH (A4H9Q9). The validity of the peptide-spectra matches (PSMs) generated by COMET was assessed using Patternlab´s module SEPro[35] with a false discovery rate of 1% based on the number of decoys.

Oligomeric state determination

Determination of *Lb*IU-NH molecular mass in solution was determined by size exclusion liquid chromatography on a HighLoad 10/30 Superdex-200 column (GE Healthcare), injecting 100 µL of protein suspension (7 µM homogeneous recombinant protein) at 0.4 mL min^{-1} flow rate and isocratic elution with 1 CV of 50 mM Tris HCl pH 7.5 containing 200 mM NaCl. Protein elution was monitored at 215, 254 and 280 nm. The LMW and HMW Gel Filtration Calibration Kits (GE Healthcare) were used to prepare a calibration curve. The values of elution volumes (V_e) of protein standards (ferritin, aldolase, conalbumin, ovalbumin, ribonuclease A and carbonic anhydrase) were used to calculate their corresponding partition coefficient (K_{av}). The latter values were plotted against the logarithm of the molecular mass of standards, and the resulting linear function employed to obtain an estimate *Lb*IU-NH molecular mass in solution. The K_{av} values were determined from Eq. 1. Blue dextran 2000 (GE Healthcare) was used to determine the void volume (V_0). V_t is the total bed volume of the column.

$$K_{AV} = \frac{V_e - V_0}{V_t - V_0} \qquad \text{Equation 1}$$

Steady-state kinetics parameters

Recombinant *Lb*IU-NH enzyme activity was measured by a continuous spectrophotometric assay in quartz cuvettes (1 cm) using a UV-visible Shimadzu spectrophotometer UV2550 equipped with a temperature-controlled cuvette holder. Kinetic properties of *Lb*IU-NH for inosine were spectrophotometrically determined using the difference in absorption between the nucleoside and the purine base. Enzyme activity was measured in the presence of varying concentrations of inosine (0.2 mM - 1.5 mM) in 50 mM Tris HCl pH 7.5 at 25 °C. The reaction was started with addition of 5 µL of recombinant *Lb*IU-NH (80 nM final concentration) that resulted in decreasing linear absorbance time courses for the conversion of nucleoside substrate into products; all assays were performed at least in duplicate. The $\Delta\varepsilon$ value employed was 0.92 mM^{-1} cm^{-1} at 280 nm.[16] The experimental data were either fitted to Michaelis-Menten equation (Eq. 2) for a hyperbolic saturation curve,[37;38] in which *v* is

the initial velocity, V is the apparent maximum initial velocity, *A* is the varying substrate concentration, and K_M represents the apparent Michaelis-Menten constant.

$$v = \frac{VA}{K_M + A} \qquad \text{Equation 2}$$

The k_{cat} values were calculated from Eq. 3, in which $[E]_t$ corresponds to the total concentration of *Lb*IU-NH enzyme subunits.

$$k_{cat} = \frac{V}{[E]_t} \qquad \text{Equation 3}$$

As no saturation for the uridine reaction could be detected by the continuous spectrophotometric assay, reversed-phase HPLC using a Dionex Ultimate 3000 with UV/VIS detector was employed to monitor the conversion of uridine into uracil. Briefly, assay mixtures containing Tris HCl 50mM pH 7.5, 40 nM of *Lb*IU-NH various uridine concentrations (1 mM - 7.0 mM) were incubated at 25 °C. At seven time intervals (1, 3, 5, 7.5, 10 12.5 and 15 min), solutions were boiled for 3 min to stop the reaction and centrifuged at 10,600 × g for 3 min. No enzyme activity could be detected for adenosine, guanosine and cytidine by the continuous spectrophotometric assay. Accordingly, the HPLC discontinuous assay was also employed to detect *Lb*IU-NH enzyme activity, if any, for these substrates with some minor modifications: assay mixtures contained Tris HCl 50 mM pH 7.5, 136 nM of *Lb*IU-NH, and either adenosine (0.25 - 4.0 mM), guanosine (0.2 - 2.0 mM), or cytidine (0.5 - 4.5 mM) were incubated at 25 °C at 6 time intervals (5, 10, 15, 20, 30 and 40 min) of reaction, after which solutions were boiled for 3 min and centrifuged at 10 600 × g for 3 min.

The supernatant (10 µL) for each reaction was injected onto a reversed-phase Nucleodur 100-5 C-18 HPLC column (250 x 4.6 mm, Macherey-Nagel). The mobile phase was ammonium acetate 10 mM (Merck®, Darmstadt, Germany) with a flow rate of 0.5 mL min^{-1}. Elution of substrate and product was monitored at 254 nm, and the integrated peak area of product was compared to standard solutions to calculate the concentration of product formed at a specific time interval, yielding initial velocity values. The results were fitted either to Michaelis-Menten (Eq. 2) for hyperbolic curves or to the Hill equation (Eq. 4) for sigmoidal curves.[37;38] For Eq. 4, *v* represents the initial velocity, V is the apparent maximum initial velocity, *A* is the varying substrate concentration, $K_{0.5}$ is the substrate concentration in which the velocity is half of the maximum velocity and *n* is the Hill coefficient.

$$v = \frac{V[A]^n}{K_{0.5}^n + [A]^n} \qquad \text{Equation 4}$$

One unit of enzyme activity (U) was defined as the amount of enzyme catalyzing the conversion of 1 µmol of substrate into product per minute at 25 °C.

Isothermal titration calorimetry

ITC experiments were carried out using an iTC_{200} Microcalorimeter (Microcal, Inc., Pittsburgh, USA). Reference cell (200 µL) was loaded with Milli-Q water during all experiments and sample cell (200 µL) was filled with 100 µM of *Lb*IU-NH recombinant enzyme in Tris HCl 50mM pH 7.5. The injection syringe (39.7 µL) was filled with the products at different concentrations: Ribose at 10 mM, Hypoxanthine and Uracil at 5 mM using the same buffer to prepare all ligand solutions. Ligand binding isotherms were measured by direct titration (ligand into macromolecule). The stirring speed was 500 RPM at 25 °C with constant pressure for all ITC experiments. The binding reaction started with one injection of 0.5 µL followed by 19 injections of 2.0 µL each at 300 s intervals. Control titrations (ligand into buffer) were performed in order to subtract the heats of dilution and mixing for each experiment prior to data analysis. ITC data were fitted to Eq. 5, in which ΔH is the enthalpy of binding, ΔG is the Gibbs free energy change, ΔS is the entropy change, *T* is the absolute temperature in Kelvin, *R* is the gas constant (1.987 cal K^{-1} mol^{-1}) and K_a is the equilibrium association constant. The dissociation constant, K_d, was calculated as the inverse of K_a (Eq. 6). All data were evaluated using the Origin 7 SR4 software (Microcal, Inc.)

$$\Delta G = \Delta H - T\Delta S = -RT\ln K_a \qquad \text{Equation 5}$$

$$K_d = \frac{1}{K_a} \qquad \text{Equation 6}$$

Energy of activation

The energy of activation (E_a) was assessed by measuring k_{cat} values of *Lb*IU-NH as a function of increasing temperature. Initial velocities were measured in the presence of fixed-saturating concentration of inosine (1.4 mM) at temperatures ranging from 15 to 35 °C (from 288.15 to 308.15 K). Prior to data collection, *Lb*IU-NH was incubated for several minutes in all tested temperatures and assayed under standard conditions to verify enzyme stability. All assays were performed in duplicates. E_a was calculated from the slope (E_a/R) of the Arrhenius plot fitting the data to Eq. 7, in which R is the gas constant (8.314 J mol^{-1} K^{-1}) and the constant A represents the product of the collision frequency (Z), and a steric factor (p) based on the collision theory of enzyme kinetics.[39] A simplistic approach was adopted to explain a complex phenomenon and that A is independent of temperature.

$$\ln k_{cat} = \ln A - \left(\frac{E_a}{R}\right)\frac{1}{T} \qquad \text{Equation 7}$$

The enthalpy ($\Delta H^{\#}$), entropy ($\Delta S^{\#}$), and Gibbs free energy ($\Delta G^{\#}$) of activation were estimated using the following equations (Eqs. 8-10) derived from the transition state theory of enzymatic reactions.[39]

$$\Delta H^{\#} = E_a - RT \qquad \text{Equation 8}$$

$$\Delta G^{\#} = RT\left(\ln\frac{k_B}{h} + \ln T - \ln k_{cat}\right) \qquad \text{Equation 9}$$

$$\Delta S^{\#} = \frac{\Delta H^{\#} - \Delta G^{\#}}{T} \qquad \text{Equation 10}$$

Energy values are in kJ mol^{-1}, with k_{cat} in s^{-1}, to conform to the units of the Boltzmann (k_b) (1.3805 × 10^{-23} J K^{-1}) and Planck (h) (6.6256 × 10^{-34} J s^{-1}) constants, and R is as for Eqs. 8 and 9. Errors on $\Delta G^{\#}$ were calculated using Eq. 11.[39]

$$(\Delta G)_{Err} = \frac{RT(k_{cat})_{Err}}{k_{cat}} \qquad \text{Equation 11}$$

Solvent kinetic isotope effects (SKIE) and proton inventory

Solvent kinetic isotope effects were determined by measuring initial velocities of *Lb*IU-NH in presence of varying concentrations of inosine (0.2 mM to 1.4 mM) in either H_2O or 90 % D_2O in 50 mM Tris HCl pH 7.5 buffer. The proton inventory was assessed at fixed-saturating concentration of inosine (1.4 mM) with various mole fractions of D_2O (0 - 90%) in 50 mM Tris HCl pH 7.5 buffer. Data were fitted to Eq. 12, which assumes isotope effects on both V/K and V. In this equation, $E_{v/k}$ and E_v are the isotope effects minus 1 on V/K and V, respectively, and F_i is the fraction of isotopic label in substrate A.[40]

$$v = \frac{VA}{K(1 + F_i E_{V/K}) + A(1 + F_i E_V)} \qquad \text{Equation 12}$$

pH-rate profiles

The dependence of kinetic parameters on pH was determined by measuring initial velocities in the presence of varying inosine concentrations (0.2 mM – 1.4 mM) in 100 mM 2-(*N*-morpholino) ethanesulfonic acid (MES)/*N*-2-hydroxyethylpiperazine-*N*-2-ethanesulfonic acid (HEPES)/2-(*N*-cyclohexylamino) ethanesulfonic acid (CHES) buffer mixture over the following pH values: 5.0, 6.0, 6.5, 7.0, 7.5, 8.0 and 8.5.[39] All measurements were carried out at least in duplicates. The pH-rate profile was generated by plotting logarithm value of k_{cat} or k_{cat}/K_M of the substrate versus pH values. The data were fitted to either Eq. 13 or 14, in which y is the apparent kinetic parameter, C is the pH-independent plateau value of y, H is the hydrogen ion concentration, and K_a and K_b are, respectively, the apparent acid and base dissociation constant for the ionizing group. Prior to performing the pH-rate profiles, *Lb*IU-NH was incubated for 2 min at 25 °C over a broader pH range in either 100 mM citrate or CHES buffer and enzyme activity was measured in assay mixtures containing inosine (1.4 mM) in

Tris HCl 50 mM pH 7.5 buffer. These measurements were carried out to show whether changes in enzyme activity were due to changes in proton concentration or to protein denaturation.

Eq. 13 describes a bell-shaped pH profile for a group that must be protonated for binding/catalysis and another group that must be unprotonated for binding/catalysis, and participation of a single ionizing group for the acidic limb (slope value of +1) and participation of a single ionizing group for the basic limb (slope value of -1).

$$\log y = \log\left(\frac{C}{1+\frac{H}{K_a}+\frac{K_b}{H}}\right) \qquad \text{Equation 13}$$

Eq. 14 describes a pH profile for a group that must be unprotonated for binding/catalysis and participation of a single ionizing group for the acidic limb (slope value of +1).

$$\log y = \log\left(\frac{C}{1+\frac{H}{K_a}}\right) \qquad \text{Equation 14}$$

Pre-steady-state kinetics

Pre-steady-state kinetic parameters of the reaction catalyzed by *Lb*IU-NH were determined using an Applied Photophysics SX.18MV-R stopped-flow spectrofluorimeter on absorbance mode to assess whether product release is part of the rate-limiting step. The decrease in absorbance was monitored at 280 nm for 0.5 s collecting 400 points (1 mm slit width = 4.65 nm spectral band) and an optical path of 2 mm. The experimental conditions were 10 μM of *Lb*IU-NH, 2 mM of inosine in Tris HCl 50 mM pH 7.5 (mixing chamber concentrations). The control experiments were performed as the experimental conditions above in the absence of enzyme. The dead time of the equipment is 1.37 ms.

The pre-steady-state time course of the reaction was fitted to Eq. 15 for a linear decay, in which A is the absorbance at time t, A_0 is the absorbance at time zero, and k is the apparent first order rate constant for product formation.[41]

$$A = A_0 + kt \qquad \text{Equation 15}$$

Crystal structure determination

Crystals were obtained by sitting-drop vapor diffusion at 291 K in a solution containing 0.2 M Ammonium acetate, 0.1 M HEPES pH 7.5 and 45 % 2-methyl-2,4-pentanediol (MPD). The addition of 10 % ethylene glycol to the original crystal growth conditions was used for cryoprotection. Diffraction data from crystals of *Lb*IU-NH were collected on beamline MX2 at LNLS equipped with a Pilatus 2M detector using a wavelength of 1.459 Å, an oscillation range of 0.3 ^{o} and a 3 s exposure time per image at 100 K. The data were indexed, integrated and scaled using the programs iMOSFLM[42] and SCALA[43] from the CCP4 suite.[42;44] The asymmetric unit was estimated with respective Matthews' coefficients.[45;46] The phase problem was solved by molecular replacement using MOLREP program.[43] The search model employed was the structure of IU-NH from *Leishmania major* (PDB access code 1EZR, subunit A). The structure was refined using Phenix.refine[47;48] (10% of the reflections for the calculation of R_{free} parameter) and Coot for model building[49] using σ_a-weighted $2F_o$-F_c and F_o-F_c electron-density maps. The parameters R and R free were used as the principal criterion for validating the refinement protocol and the stereochemical quality of the model was evaluated with PROCHECK[50] and MolProbity.[51] The final protein concentration of *Lb*IU-NH for crystallization was 2.7 mg mL^{-1}. The solution also contained solution of 10 mM of D-(-)-ribose (linear), whereas a β-D-ribose (ribofuranosidic form) was found in the *Lb*IU-NH structure. We have employed this crystallization strategy to take advantage of mutarotation processes. Mutarotation is known to occur with monosacharides as there is an equilibrium between open, α and β anomeric forms. The simple linear form is assumed to be the intermediate of four species of D-ribose: α-furan (7.1 %), β-furan (12.3 %), α-pyran (22.4 %), and β-pyran (58.2 %).[51] The spontaneous α-to-β exchange rate constants of furanosidic forms are at least one-order of magnitude higher than the pyranosidic forms.[52] It is thus likely that *Lb*IU-NH

bound the β-furanosidic form due to its larger percentage in solution and/or due to its larger affinity constant. The atomic coordinates were deposited in the Protein Data Bank, PDB ID code 5TSQ.

Acknowledgements

This work was supported by funds awarded by Decit/SCTIE/ MSMCT-CNPq-FNDCT-CAPES to National Institute of Science and Technology on Tuberculosis (INCT-TB) to D.S.S. and L.A.B. L.A.B. (CNPq, 520182/99-5), D.S.S. (CNPq, 304051/1975-06), O.N.S. (CNPq, 305984/2012-8), and E.M.C.F. (CNPq, 306706/2014-8) are Research Career Awardees of the National Research Council of Brazil (CNPq). P.F.D. acknowledges a scholarship awarded by CAPES. L.K.B.M. is a Post-Doctoral Fellow of FAPERGS/CAPES.

Conflict of interest

The authors declare that they have no conflicts of interest with the contents of this article.

Author contributions

PFD and LKBM designed, performed and analyzed all biochemical experiments, and drafted the paper. JFRB, LFSMT and ONS crystallized and solved the X-ray structure of *Lb*IU-NH. CVB, LG, FTS and ADV designed vectors, and performed cloning and expression. AFPM and CVB designed, performed and analyzed the mass spectrometry experiments. ASD and GOP designed and performed HPLC method. KP and PM carried out the spectroscopic experiments. FTS also contributed to writing and formatting the manuscript. EMCF, LAB and DSS designed experiments and revised critically the manuscript.

References

1 Shaw, J. J. (2006) Further thoughts on the use of the name *Leishmania (Leishmania) infantum chagasi* for the aetiological agent of American visceral leishmaniasis. *Mem Inst Oswaldo Cruz* **101**, 577-579

2 Teixeira, D. E., Benchimol, M., Rodrigues, J. C. F., Crepaldi, P. H., Pimenta, P. F. P., and de Souza, W. (2013) *Atlas Didático Ciclo de vida da Leishmania* 1st ed., Fundação CECIERJ, Rio de Janeiro, Brazil.

3 Who. (2010) World Health Organization - Control of the leishmaniases. World Health Organization, Geneva

4 Martin, J. L., Yates, P. A., Soysa, R., Alfaro, J. F., Yang, F., Burnum-Johnson, K. E., Petyuk, V. A., Weitz, K. K., Camp, D. G., Smith, R. D., Wilmarth, P. A., David, L. L., Ramasamy, G., Myler, P. J., and Carter, N. S. (2014) Metabolic reprogramming during purine stress in the protozoan pathogen *Leishmania donovani*. *PLoS Pathog* **10**, e1003938

5 Cui, L., Rajasekariah, G. R., and Martin, S. K. (2001) A nonspecific nucleoside hydrolase from *Leishmania donovani*: implications for purine salvage by the parasite. *Gene* **280**, 153-162

6 Alvar, J., Vélez, I. D., Bern, C., Herrero, M., Desjeux, P., Cano, J., Jannin, J., den Boer, M., the WHO Leishmaniasis Control Team. (2012) Leishmaniasis worldwide and global estimates of its incidence. *PLoS One* **7**, e35671

7 Marsden, P. D. (1985) Pentavalent antimonials: old drugs for new diseases. *Revista da Sociedade Brasileira de Medicina Tropical* **18**, 187-198

8 Frézard, F., Demicheli, C., and Ribeiro, R. R. (2009) Pentavalent antimonials: new perspectives for old drugs. *Molecules* **14**, 2317-2336

9 Berman, J. D. (1997) Human Leishmaniasis: Clinical, Diagnostic, and Chemotherapeutic Developments in the Last 10 Years. *Clin Infect Dis* **24**, 684-703

10 Meyerhoff, A. (1998) U.S. Food and Drug Administration Approval of AmBisome (Liposomal Amphotericin B) for Treatment of Visceral Leishmaniasis. *Clin Infect Dis* **28**, 42-48

11 Sundar, S., Jha, T. K., Thakur, C. P., Engel, J., Sindermann, H., Fischer, C., Junge, K., Bryceson, A., and Berman, J. (2002) Oral miltefosine for Indian visceral leishmaniasis. *N Engl J Med* **347**, 1739-1746

12 LaFon, S. W., Nelson, D. J., Berens, R. L., and Marr, J. J. (1982) Purine and pyrimidine salvage pathways in *Leishmania donovani*. *Biochem Pharmacol* **31**, 231-238

13 Marr, J. J., Berens, R. L., and Nelson, D. J. (1978) Purine metabolism in *Leishmania donovani* and *Leishmania braziliensis*. *Biochim Biophys Acta* **544**, 360-371

14 Boitz, J. M., Ullman, B., Jardim, A., and Carter, N. S. (2012) Purine salvage in Leishmania: complex or simple by design? *Trends Parasitol* **28**, 345-352

15 Versées, W., Van Holsbeke, E., De Vos, S., Decanniere, K., Zegers, I., and Steyaert, J. (2003) Cloning, preliminary characterization and crystallization of nucleoside hydrolases from *Caenorhabditis elegans* and *Campylobacter jejuni*. *Acta Cryst* **D59**, 1087-1089

16 Parkin, D. W., Horenstein, B. A., Abdulah, D. R., Estupiñán, B., and Schramm, V. L. (1991) Nucleoside hydrolase from *Crithidia fasciculata*. Metabolic role, purification, specificity, and kinetic mechanism. *J Biol Chem* **266**, 20658-20665

17 Shi, W., Schramm, V. L., and Almo, S. C. (1999) Nucleoside hydrolase from *Leishmania major*. Cloning, expression, catalytic properties, transition state inhibitors, and the 2.5-Å crystal structure. *J Biol Chem* **274**, 21114-21120

18 Iovane, E., Giabbai, B., Muzzolini, L., Matafora, V., Fornili, A., Minici, C., Giannese, F., and Degano, M. (2008) Structural basis for substrate specificity in group I nucleoside hydrolases. *Biochemistry* **47**, 4418-4426

19 Horenstein, B. A., and Schramm, V. L. (1993) Electronic nature of the transition state for nucleoside hydrolase. A blueprint for inhibitor design. *Biochemistry* **32**, 7089-7097

20 Degano, M., Gopaul, D. N., Scapin, G., Schramm, V. L., and Sacchettini, J. C. (1996) Three-dimensional structure of the inosine-uridine nucleoside N-ribohydrolase from *Crithidia fasciculata*. *Biochemistry* **35**, 5971-5981

21 Miller, R. L., Sabourin, C. L., Krenitsky, T. A., Berens, R. L., and Marr, J. J. (1984) Nucleoside hydrolases from *Trypanosoma cruzi*. *J Biol Chem* **259**, 5073-5077

22 Horenstein, B. A., Parkin, D. W., Estupiñán, B., and Schramm, V. L. (1991) Transition-state analysis of nucleoside hydrolase from *Crithidia fasciculata*. *Biochemistry* **30**, 10788-10795

23 Wink, P. L., Sanchez Quitian, Z. A., Rosado, L. A., Rodrigues, V. a. S., Petersen, G. O., Lorenzini, D. M., Lipinski-Paes, T., Timmers, L. F. S. M., de Souza, O. N., Basso, L. A., and Santos, D. S. (2013) Biochemical characterization of

recombinant nucleoside hydrolase from *Mycobacterium tuberculosis* H37Rv. *Arch Biochem Biophys* **538**, 80-94

24 Versées, W., Decanniere, K., Pellé, R., Depoorter, J., Brosens, E., Parkin, D. W., and Steyaert, J. (2001) Structure and function of a novel purine specific nucleoside hydrolase from *Trypanosoma vivax*. *J Mol Biol* **307**, 1363-1379

25 Ladbury, J. E., Doyle, M. L., and Doyle, M. L. B. (2004) *Biocalorimetry 2: applications of calorimetry in the biological sciences*, John Wiley, Chichester

26 Northrop, D. B. (1975) Steady-state analysis of kinetic isotope effects in enzymic reactions. *Biochemistry* **14**, 2644-2651

27 Gopaul, D. N., Meyer, S. L., Degano, M., Sacchettini, J. C., and Schramm, V. L. (1996) Inosine-uridine nucleoside hydrolase from *Crithidia fasciculata*. Genetic characterization, crystallization, and identification of histidine 241 as a catalytic site residue. *Biochemistry* **35**, 5963-5970

28 Degano, M., Almo, S. C., Sacchettini, J. C., and Schramm, V. L. (1998) Trypanosomal nucleoside hydrolase. A novel mechanism from the structure with a transition-state inhibitor. *Biochemistry* **37**, 6277-6285

29 Psoda, A., and Shugar, D. (1971) Spectral studies on tautomeric forms of inosine. *Biochim. Biophys. Acta* **247**, 507-513

30 Giabbai, B., and Degano, M. (2004) Crystal structure to 1.7 a of the *Escherichia coli* pyrimidine nucleoside hydrolase YeiK, a novel candidate for cancer gene therapy. *Structure* **12**, 739-749

31 Yang, W., Lee, H.-W., Hellinga, H., and Yank, J. J. (2002) Structural Analysis, Identification, and Design of Calcium-Binding Sites in Proteins. *Proteins: Structure, Function, and Genetics* **47**, 344-356

32 Pidcock, E., and Moore, G. R. (2001) Structural characteristics of protein binding sites for calcium and lanthanide ions. *J Biol Inorg Chem* **6**, 479-489

33 Fornili, A., Giabbai, B., Garau, G., and Degano, M. (2010) Energy landscapes associated with macromolecular conformational changes from endpoint structures. *J Am Chem Soc* **132**, 17570-17577

34 Shevchenko, A., Tomas, H., Havlis, J., Olsen, J. V., and Mann, M. (2006) In-gel digestion for mass spectrometric characterization of proteins and proteomes. *Nat Protoc* **1**, 2856-2860

35 Carvalho, P. C., Lima, D. B., Leprevost, F. V., Santos, M. D., Fischer, J. S., Aquino, P. F., Moresco, J. J., Yates, J. R., and Barbosa, V. C. (2016) Integrated analysis of shotgun proteomic data with PatternLab for proteomics 4.0. *Nat Protoc* **11**, 102-117

36 Eng, J. K., Jahan, T. A., and Hoopmann, M. R. (2013) Comet: an open-source MS/MS sequence database search tool. *Proteomics* **13**, 22-24

37 Copeland, R. A. (2005) Evaluation of enzyme inhibitors in drug discovery : a guide for medicinal chemists and pharmacologists, John Wiley, Hoboken, N.J.; Chichester

38 Segel, I. H. (1975) Enzyme Kinetics: Behavior and Analysis of Rapid Equilibrium and Steady-State Enzyme Systems, Wiley-Interscience, New York

39 Lonhienne, T., Baise, E., Feller, G., Bouriotis, V., and Gerday, C. (2001) Enzyme activity determination on macromolecular substrates by isothermal titration

calorimetry: application to mesophilic and psychrophilic chitinases. *Biochim Biophys Acta* **1545**, 349-356

40 Cook, P. F., and Cleland, W. W. (2007) *Enzyme kinetics and mechanism*, Garland Science, London and New York

41 Hiromi, K. (1979) Kinetics of Fast Enzyme Reactions: Theory and Practice, Kodansha Ltd., Tokyo

42 Battye, T. G., Kontogiannis, L., Johnson, O., Powell, H. R., and Leslie, A. G. (2011) iMOSFLM: a new graphical interface for diffraction-image processing with MOSFLM. *Acta Cryst* **D67**, 271-281

43 Winn, M. D., Ballard, C. C., Cowtan, K. D., Dodson, E. J., Emsley, P., Evans, P. R., Keegan, R. M., Krissinel, E. B., Leslie, A. G. W., McCoy, A., McNicholas, S. J., Murshudov, G. N., Pannu, N. S., Potterton, E. A., Powell, H. R., Read, R. J., Vagin, A., and Wilson, K. S. (2011) Overview of the CCP4 suite and current developments. *Acta Cryst* **D67**, 235-242

44 Leslie, A. G. (2006) The integration of macromolecular diffraction data. *Acta Cryst* **D62**, 48-57

45 Matthews, B. W. (1968) Solvent content of protein crystals. *J Mol Biol* **33**, 491-497

46 Kantardjieff, K. A., and Rupp, B. (2003) Matthews coefficient probabilities: Improved estimates for unit cell contents of proteins, DNA, and protein-nucleic acid complex crystals. *Protein Sci* **12**, 1865-1871

47 Adams, P. D., Grosse-Kunstleve, R. W., Hung, L. W., Ioerger, T. R., McCoy, A. J., Moriarty, N. W., Read, R. J., Sacchettini, J. C., Sauter, N. K., and Terwilliger, T. C. (2002) PHENIX: building new software for automated crystallographic structure determination. *Acta Cryst* **D58**, 1948-1954

48 Afonine, P. V., Grosse-Kunstleve, R. W., Echols, N., Headd, J. J., Moriarty, N. W., Mustyakimov, M., Terwilliger, T. C., Urzhumtsev, A., Zwart, P. H., and Adams, P. D. (2012) Towards automated crystallographic structure refinement with phenix.refine. *Acta Cryst* **D68**, 352-367

49 Emsley, P., Lohkamp, B., Scott, W. G., and Cowtan, K. (2010) Features and development of Coot. *Acta Cryst* **D66**, 486-501

50 Laskowski, R. A., MacArthur, M. W., and Thornton, J. M. (2001) *PROCHECK: validation of protein structure coordinates*, Kluwer Academic Publishers, The Netherlands

51 Chen, V. B., Arendall, W. B., Headd, J. J., Keedy, D. A., Immormino, R. M., Kapral, G. J., Murray, L. W., Richardson, J. S., and Richardson, D. C. (2010) MolProbity: all-atom structure validation for macromolecular crystallography. *Acta Cryst* **D66**, 12-21

52 Ryu, K-S., Kim, C., Park, C., and Choi, B-S. (2004) NMR analysis of enzyme-catalyzed and free-equilibrium mutarotation kinetics of monosaccharides. *J Am Chem Soc* **126**, 9180-9181.

Table 1 Steady-state kinetic parameters for *Lb*IU-NH

Substrate	$K_m/K_{0.5}$ (mM)	V_{max} (U mg^{-1})	k_{cat} (s^{-1})	k_{cat}/K_m (M^{-1} s^{-1})
Inosine	0.50 ± 0.04	19.6 ± 0.7	11.2 ± 0.4	2.2 (± 0.2) x 10^4
Uridine	3.2 ± 0.4	8 ± 1	4.5 ± 0.6	-
Adenosine	0.6 ± 0.1	0.069 ± 0.004	0.039± 0.002	65 ± 10
Cytidine	0.7 ± 0.07	0.115 ± 0.003	0.066 ± 0.002	94 ± 9
Guanosine				47 ± 2

Table 2 Data collection and refinement statistics for *Lb*IU-NH

Beamline	MX2 (LNLS)
Wavelength (Å)	1.45
Resolution range (Å)	21.65 (1.53)
Space group	I222
Unit cell (a and b, c; Å)	74.66, 94.08, 123.12
Unique Reflections	64501 (8569)
Multiplicity	4.3 (2.3)
Completeness (%)	98.9 (90.8)
Mean I/sigma(I)	10.0 (3.3)
Rmerge (%)	0.053 (0.431)
B_{factor} Wilson plot (Å²)	23.7
CC1/2	0.991 (0.705)
R_{work}	15.34 (18.84)
R_{free}	16.68 (20.25)
Number of atoms	
ligands	1
ions	1
waters	278
Protein residues	1023
RMS(bonds) (Å)	0.011
RMS(angles) (o)	0.972
Ramachandran favored (%)	98.6
Ramachandran outliers (%)	0
Clashscore	2.64
Average B-factors (Å²)	
Macromolecule	20.946
Ligands	20.053
Solvent	38.510
PDB code	5TSQ

FIGURE LEGENDS

FIGURE 1 Determination of kinetic parameters for *Lb*IU-NH. Specific activity/velocity plotted against increasing concentrations of (A) inosine (B) adenosine and (C) cytidine obeying the Michaelis-Menten kinetics, (D) uridine showing a sigmoidal profile, and (E) guanosine.

FIGURE 2 Ligand binding assay for α-D-ribose. The top panel represents raw data of the heat pulses and the bottom panel shows the integrated heat pulses (mol of injectant as a function of the molar ratio).

FIGURE 3 Arrhenius plot for inosine. Values for the maximum velocity of *Lb*IU-NH-catalyzed chemical reaction were determined as a function of increasing temperatures (15 to 35 °C) at fixed-saturating concentration of inosine (1.4 mM).

FIGURE 4 Solvent kinetic isotopic effects for *Lb*IU-NH. Enzyme activity was measured at increasing concentrations of inosine (0.2-1.4mM) in assay mixtures containing either 0 (●) or 90 (■) atom % D_2O. The insert represents the proton inventory (0, 20, 40, 60 or 90 atom % D_2O) with fixed-saturating concentration of inosine (1.4 mM).

FIGURE 5 Dependence of kinetic parameters on pH. (A) pH dependence of log k_{cat} data were fitted to Eq. 10; (B) pH dependence of log $k_{cat}/K_{inosine}$ data were fitted to Eq. 11.

FIGURE 6 Stopped-flow trace for product formation. Measurements of the decrease in absorbance at 280 nm due to the conversion of inosine to hypoxanthine. The data were fitted to Eq. 15 for a linear decay, yielding a value of 0.0208 s^{-1} for the apparent first-order rate constant of product formation, which corresponds to a catalytic rate constant value of 11.3 s^{-1}. The bottom stopped-flow trace represents the control experiment (absence of *Lb*IU-NH).

FIGURE 7 Overall structure of *Lb*IU-NH. (A) The quaternary structure of *Lb*IU-NH obtained from the symmetry operations of the spatial group I222. The main chains are represented as cartoon and colored by subunit: A is pale green, B is light blue, C is light red, and D is wheat. The cysteine residues involved in disulfide bonds are represented by their van der Waals raddi. (B) Calcium binding site, where the amino acids are represented as sticks and colored by CPK except by the carbon atom that is colored in green. The distances are shown in angstroms (Å). (C) Region where the disulfide bond was found, revealing a clear density map. Image generated using PyMOL.

FIGURE 1

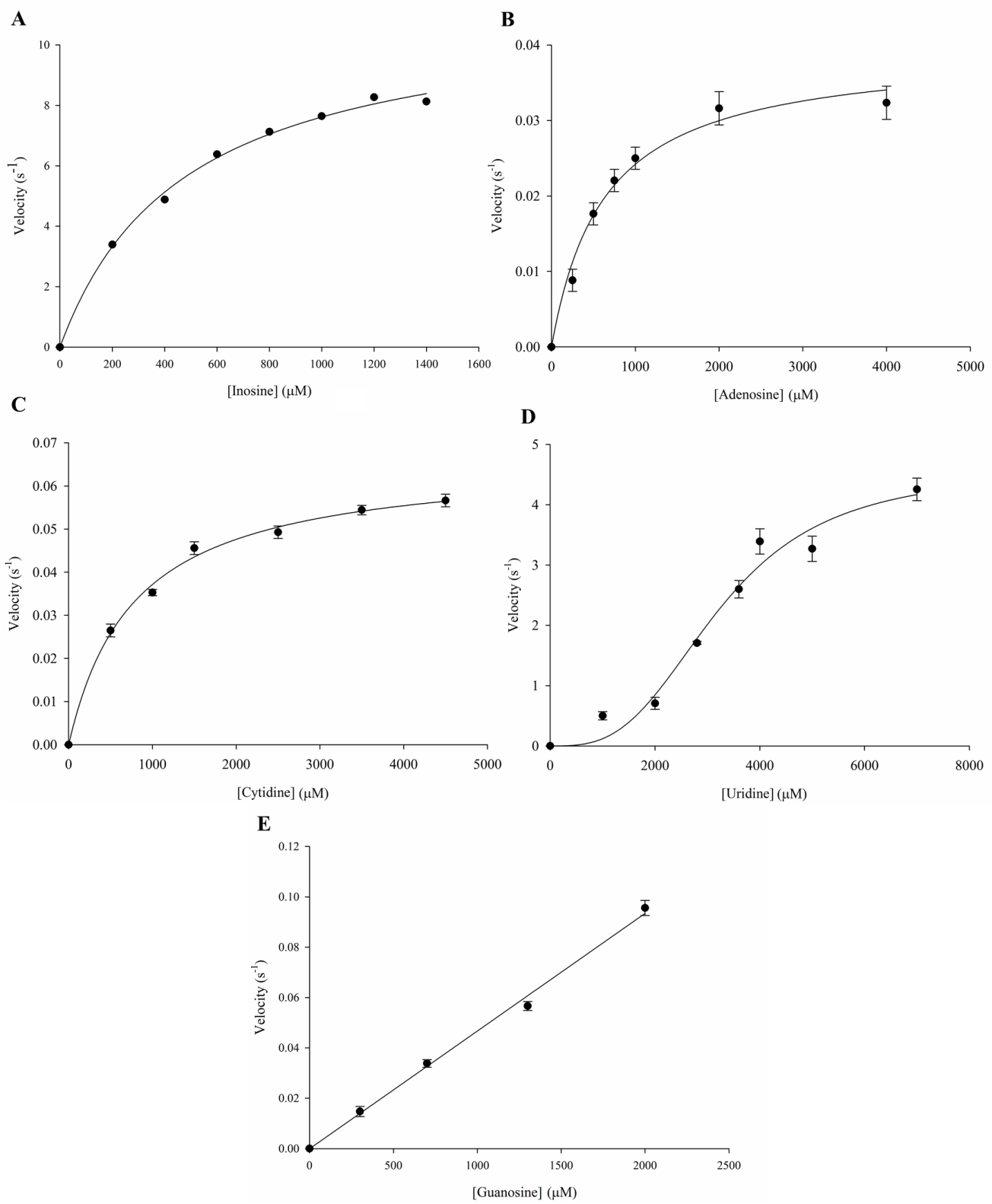
A
Velocity (s-1)
[Inosine] (μM)
B
Velocity (s-1)
[Adenosine] (μM)
C
Velocity (s-1)
[Cytidine] (μM)
D
Velocity (s-1)
[Uridine] (μM)
E
Velocity (s-1)
[Guanosine] (μM)

FIGURE 2

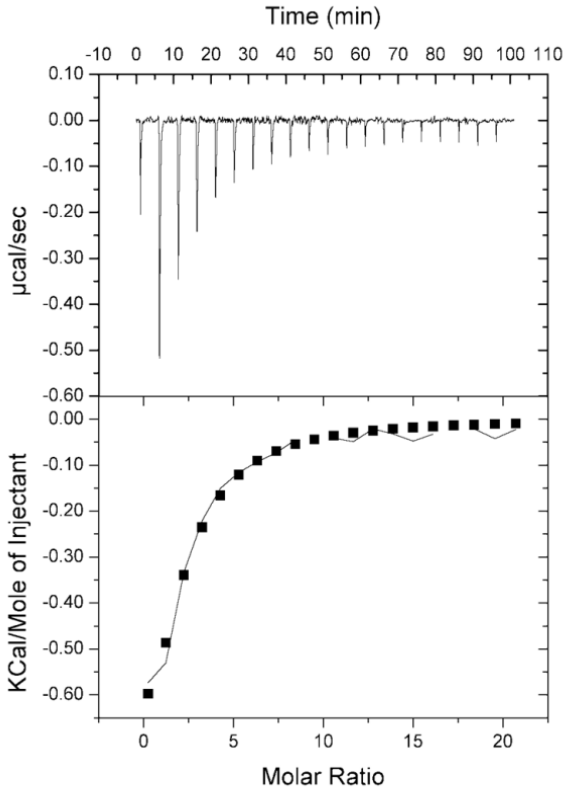
Time (min)
-10 0 10 20 30 40 50 60 70 80 90 100 110
0.10
0.00
-0.10
-0.20
-0.30
-0.40
-0.50
-0.60
µcal/sec
0.00
-0.10
-0.20
-0.30
-0.40
-0.50
-0.60
KCal/Mole of Injectant
0
5
10
15
20
Molar Ratio

FIGURE 3

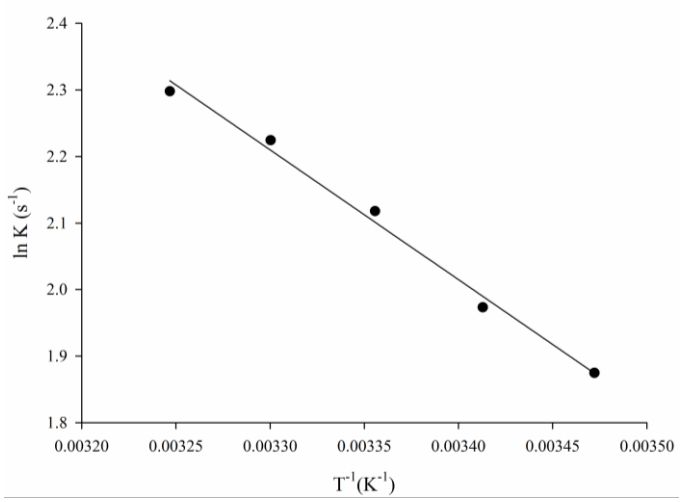
2.4
2.3
2.2
2.1
2.0
1.9
1.8
ln K (s-1)
0.00320
0.00325
0.00330
0.00335
0.00340
0.00345
0.00350
T-1(K-1)

FIGURE 4

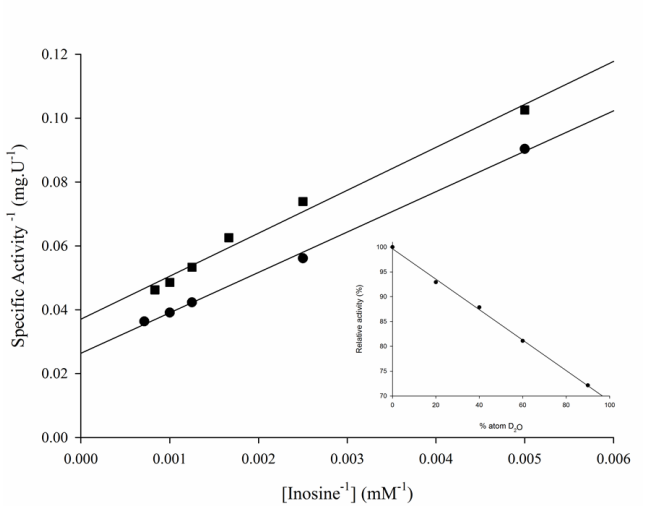
0.12
0.10
0.08
0.06
0.04
0.02
0.00
Specific Activity -1 (mg.U-1)
0.000
0.001
0.002
0.003
0.004
0.005
0.006
[Inosine-1] (mM-1)
100
95
90
85
80
75
70
Relative activity (%)
0
20
40
60
80
100
% atom D2O

FIGURE 5

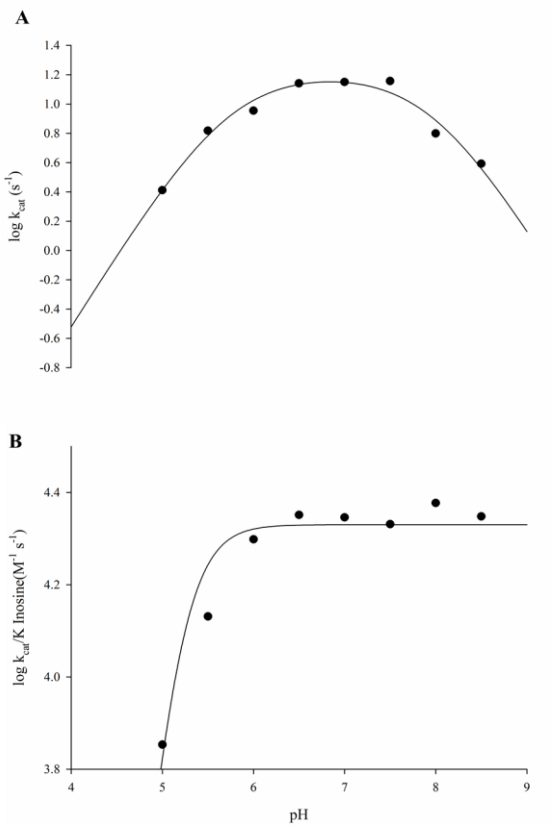
A
1.4
1.2
1.0
0.8
0.6
0.4
0.2
0.0
-0.2
-0.4
-0.6
-0.8
log k_{cat} (s^{-1})
B
4.4
4.2
4.0
3.8
log k_{cat}/K Inosine(M^{-1} s^{-1})
4
5
6
7
8
9
pH

FIGURE 6

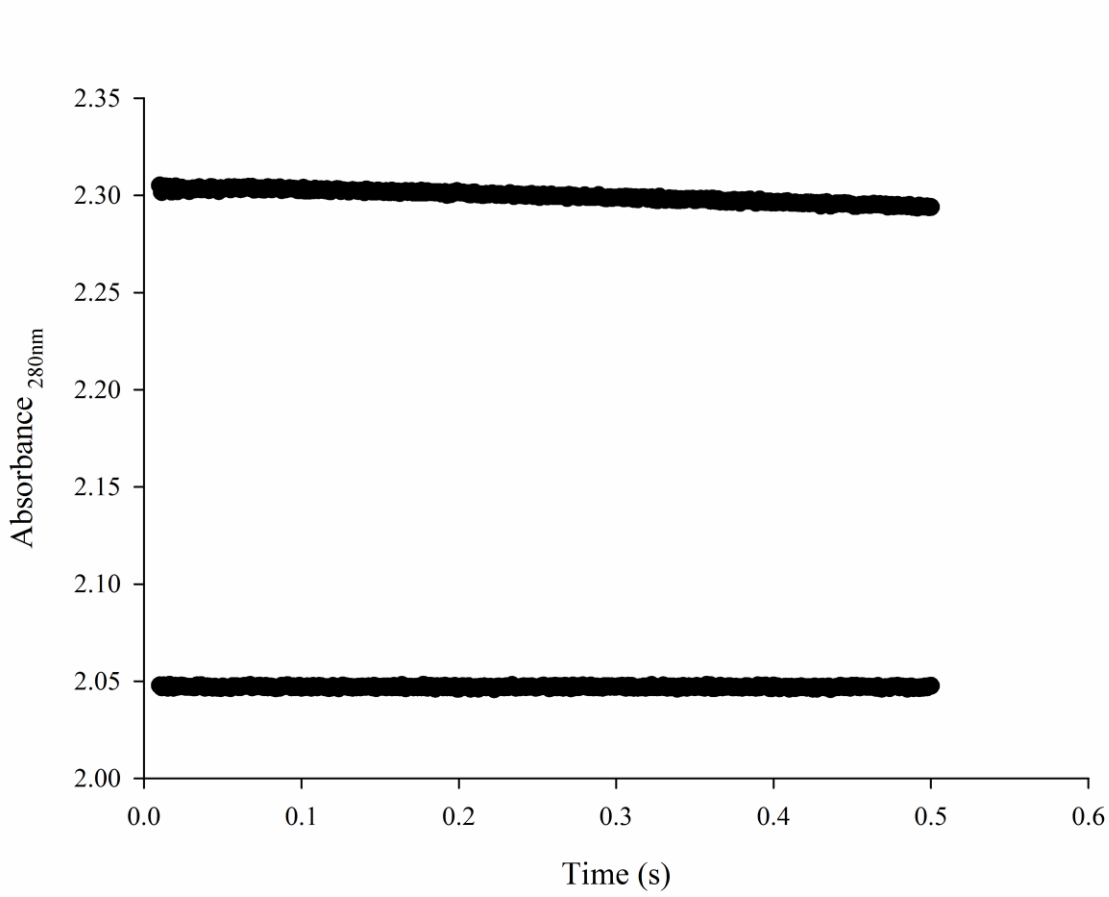
2.35
2.30
2.25
2.20
2.15
2.10
2.05
2.00
Absorbance 280nm
0.0
0.1
0.2
0.3
0.4
0.5
0.6
Time (s)

FIGURE 7

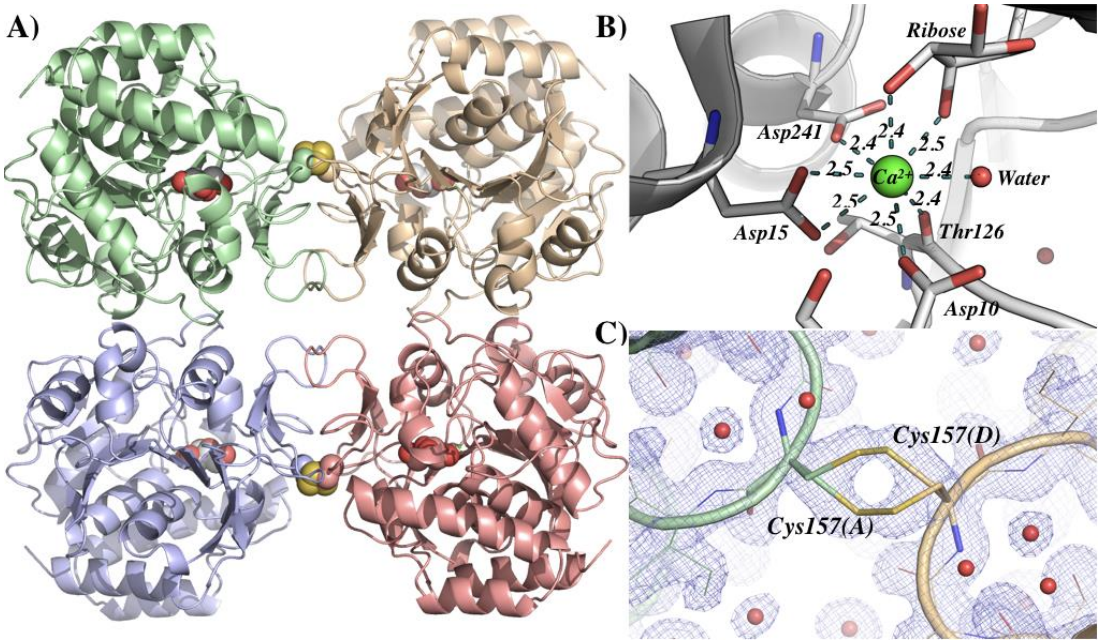
A)
B)
Ribose
Asp241
2.4
2.4
2.5
2.5
Ca2+
2.4
Water
2.5
2.4
2.5
Asp15
Thr126
Asp10
C)
Cys157(D)
Cys157(A)

Supplemental Data

Thermodynamics, Functional and Structural Characterization of Inosine-Uridine Nucleoside Hydrolase from *Leishmania braziliensis*

Pedro Ferrari Dalberto[‡], Leonardo Kras Borges Martinelli[‡], Jose Fernando Ruggiero Bachega[§], Luis Fernando Saraiva Macedo Timmers[§], Antonio Frederico Michel Pinto[‡], Adilio da Silva Dadda[‡], Guilherme Oliveira Petersen[‡], Fernanda Teixeira Subtil[‡], Luiza Galina[‡], Anne Drumond Villela[‡], Kenia Pissinate[‡], Pablo Machado[‡], Cristiano Valim Bizarro[‡], Osmar Norberto de Souza[§], Edgar Marcelino de Carvalho Filho[¶], Luiz Augusto Basso[‡1], and Diogenes Santiago Santos[‡1]

From [‡]Centro de Pesquisas em Biologia Molecular e Funcional (CPBMF), [§]Laboratório de Bioinformática, Modelagem e Simulação de Biossistemas (LABIO), Pontifícia Universidade Católica do Rio Grande do Sul (PUCRS), Porto Alegre 90650-001, RS, Brazil, and [¶]Hospital Universitário Professor Edgard Santos, Universidade Federal da Bahia, Salvador 40110160, BA, Brazil

Table of contents

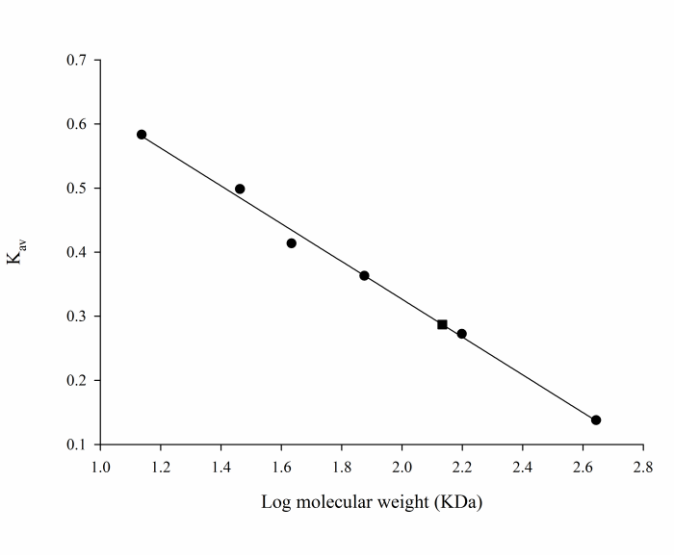

Figure S1. Determination of the oligomeric state of *Lb*IU-NH by gel filtration using a HighLoad 10/30 Superdex-200 column. Protein standards (●) were: ferritin, aldolase, conalbumin, ovalbumin, ribonuclease A and carbonic anhydrase. Blue dextran 2000 was used to determine the void volume. K_{av} was determined using Eq. 1 (main text) for each standard, and these values were plotted against logarithm of the molecular of protein standards. A value of 136,019 for the apparent molecular mass of homogeneous recombinant protein (■) was estimated suggesting that *Lb*IU-NH is a tetramer in solution.

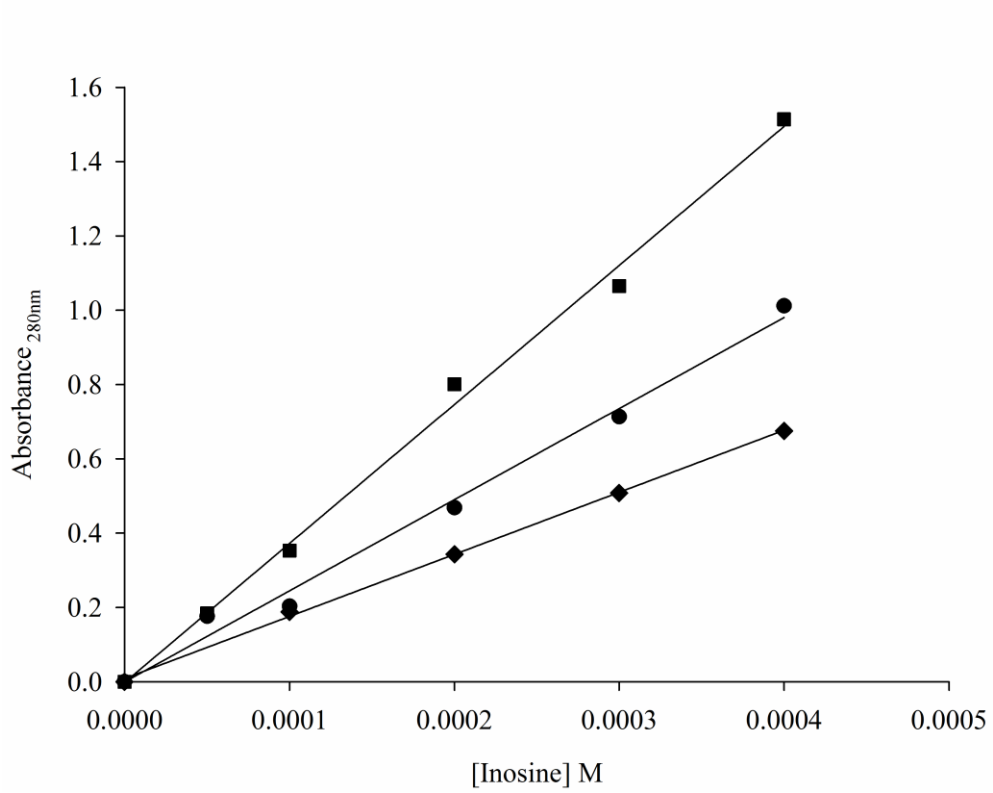

Figure S2. Molar absorptivity values at 280 nm (ε_{280}) for inosine in solvents with different dielectric constants (D). Absorbance at 280 nm were measured as a function of varying concentrations of inosine (25µM-400µM) in 50 mM Tris HCl pH 7.5 (♦), methanol (MeOH) (●) or dimethyl sulfoxide (DMSO) (■). The values for ε_{280} were: 1.7 (± 0.3) x 10^3 M^{-1} cm^{-1} for Tris HCl 50mM (D_{water} = 78.74), 2.4 (± 0.1) x 10^3 M^{-1} cm^{-1} for MeOH (D_{MeOH} = 32.6) and 3.7 (± 0.1) x 10^3 M^{-1} cm^{-1} for DMSO (D_{DMSO} = 49).

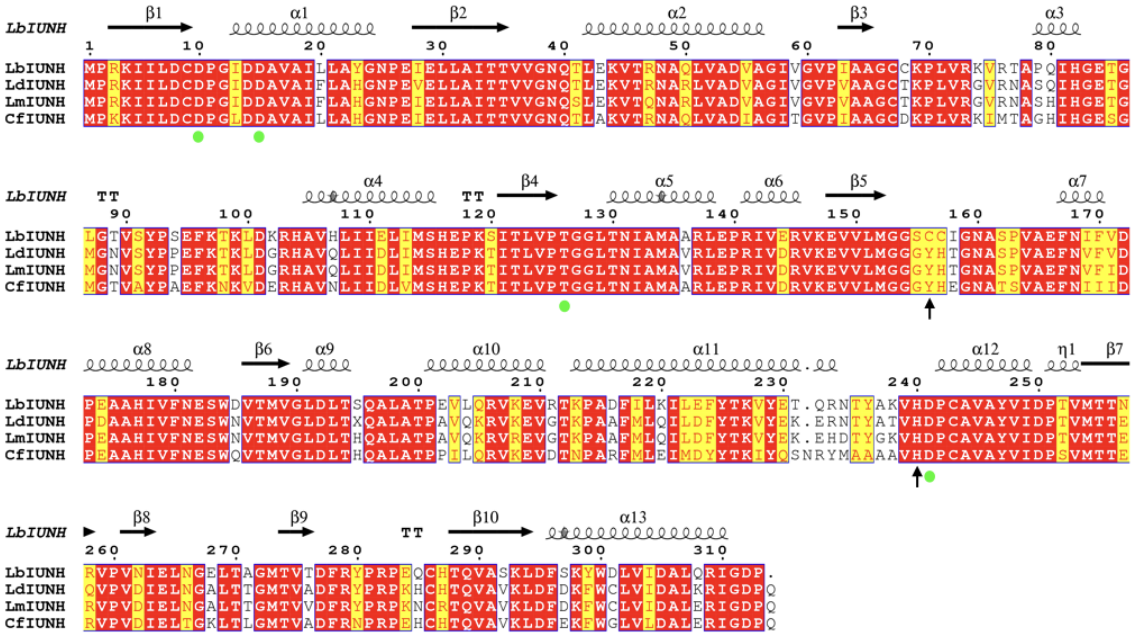

Figure S3. Primary sequence alignment of protozoan IU-NHs. The green circles are highlighting the residues responsible for anchoring the calcium ion and the arrows show the Cys157 that is involved in the disulfide bond and the residue His240. Image generated with ESPript.

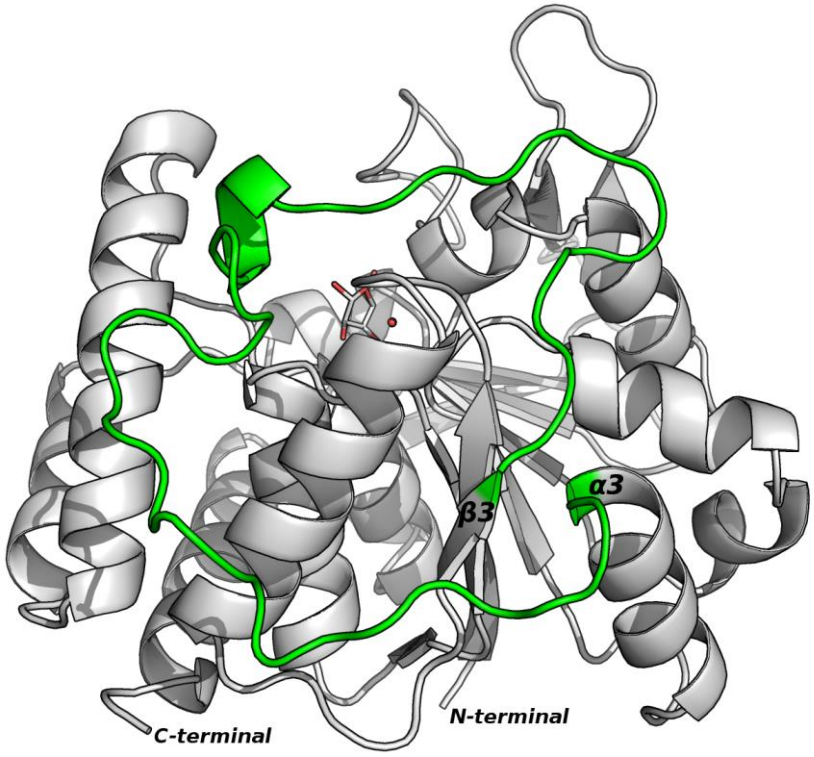

Figure S4. Overall structure of *Lb*IU-NH. The loop between β3-α3 influenced by the ligand binding is highlighted in green. Image generated with PyMOL.

Capítulo 3

Considerações Finais

4. CONSIDERAÇÕES FINAIS

A leishmaniose é uma doença infecciosa e não contagiosa, cujos agentes etiológicos são protozoários pertencentes à família Trypanosomatídae, do gênero *Leishmania*. Apesar da disponibilidade do tratamento padrão, os medicamentos apresentam muitos efeitos colaterais e são administrados por tempo prologando em ambiente hospitalar, o que leva a não aderencia do paciente ao tratamento. O desenvolvimento de novos fármacos mais eficazes, menos tóxicos, com menor duração de tratamento, e que sirvam para tratar todas as formas de leishmaniose, são necessários para diminuir a incidência global da doença. Neste contexto, as enzimas envolvidas na rota de salvamento de purinas são alvos moleculares interessantes para compostos inibidores, uma vez que *Leishmania* não possui a via de biossíntese *de novo* de nucleotídeos, e portanto, é dependente da via de salvamento de purinas para sínteses de nucleotídeos. Assim, o estudo de enzimas envolvidas nesta rota metabólica parece ser de grande importância para a descoberta e a caracterização de novos alvos moleculares para fármacos. A enzima *Lb*IU-NH pode desempenhar um papel crucial no processo de salvamento de purinas e parece ser um alvo atraente, uma vez que não existe atividade catalítica semelhante em mamíferos.

Os experimentos realizados neste trabalho incluíram a clonagem do gene *iunH* de *L. braziliensis*, a expressão da proteína recombinante em cepas de *E. coli* Rosetta (DE3) e a purificação da proteína utilizando um protocolo de três etapas cromatográficas. O seqüenciamento peptídico confirmou a identidade da proteína recombinante. A cromatografia de exclusão de tamanho sugere que a *Lb*IU-NH é um tetrâmero em solução. Os resultados de cinética em estado estacionário indicam que a enzima possui características de uma nucleosídeo hidrolase não específica, utilizando inosina, uridina, adenosina, guanosina e citidina como substrato. A uridina apresentou cinética de cooperatividade homotrópica positiva, diferente de NHs de outros protozoários, cujas curvas de saturação apresentaram somente perfil hiperbólico. A enzima apresentou baixa atividade frente aos substratos adenosina, guanosina e citidina, e através de um ensaio descontínuo utilizando cromatografia líquida de alta eficiência foi possível determinar as constantes cinéticas para cada um destes substratos.

Estudos em calorimetria de titulação isotérmica (ITC) também foram realizados, e os resultados sugerem que a ligação da α-D-ribose à enzima livre é um

processo espontâneo (ΔG inferior a 0 kcal mol^{-1}) com entalpia favorável (ΔH inferior a 0 kcal mol^{-1}) e contribuições entrópicas (ΔS maior que 0 kcal mol^{-1}). Estes dados sugerem uma redistribuição favorável de interações (ligações de hidrogênio e / ou van der Waals) e a liberação de moléculas de água no sítio ativo da enzima. Os dados também nos levaram a propor um mecanismo ordenado de liberação da base seguida pela pentose. Os parâmetros termodinâmicos de ativação para as reações catalisadas pela enzima foram determinados por meio do ensaio de energia de ativação com o substrato inosina. Verificou-se a energia necessária para que o início da reação ocorra (E_a) e os parâmetros termodinâmicos de ativação ($\Delta G^{\#}$, $\Delta S^{\#}$, $\Delta H^{\#}$). Estudos relacionados ao efeito isotópico do solvente em *V* indicam um efeito de transferência de prótons após a formação do complexo ternário, que incluem os passos químicos e possíveis alterações conformacionais da enzima e a liberação do produto. Efeito isotópico do solvente em *V/K* indicou uma modesta contribuição de transferência de prótons entre a enzima livre e o substrato até a primeira etapa irreversível. Além disso, dados de inventário de prótons sugerem que este efeito isotópico do solvente surge a partir de um único próton. O ensaio de perfil de pH para k_{cat} indicou dois grupos com o valor de pK de aproximadamente 5.2 e 7.9. O alinhamento da sequência de aminoácidos da NH de enzimas homólogas mostrou que os resíduos envolvidos na catálise estão conservados entre as NHs. A análise dos resultados obtidos com o experimento de perfil de pH, dados do alinhamento de seqüência e da estrutura nos trouxe evidências de que os aminoácidos His240 e Aps241 de *Lb*IU-NH estejam envolvidos na catálise. Além disso, os dados de pH para $k_{cat}/k_{inosina}$ indicam que um valor de pK de 5.7 é necessário para ligação da inosina, e possivelmente três resíduos de ácido aspártico (Asp10, Asp15, or Asp241) poderiam ser responsáveis por esta função. Entretanto nossos dados não conseguem distinguir qual resíduo de ácido aspártico está envolvido. Estudos do estado pré-estacionário sugerem que a liberação do produto não contribui para a etapa limitante da reação. Obtivemos a estrutura de cristalográfica da *Lb*IU-NH complexada com β-D-ribose e Ca^{+2} a 1.53 Å de resolução (PDB ID código 5TSQ). A estrutura cristalina mostrou uma ligação dissulfeto entre a interface das subunidades A-C (e B-D), que não foi encontrada em outras estruturas conhecidas de NH. Além disso, a determinação da estrutura nos possibilitou identificar os possíveis resíduos de aminoácidos relacionados com a ligação de substratos e catálise da enzima. Experimentos de caracterização cinética com a enzima contendo mutações

específicas utilizando mutagênese sítio-dirigida poderiam colaborar para a melhor compreensão do papel de resíduos aminoácidos importantes para a catálise da reação.

Este trabalho possibilitou a caracterização bioquímica e estrutural da enzima NH de *L. braziliensis* codificada pelo gene *iunH*. Os dados apresentados servirão como base para o planejamento de inibidores enzimáticos visando o desenvolvimento de novos candidatos a fármacos para a leishmaniose.

REFERÊNCIAS

1- WHO. Control of the leishmaniases: report of a meeting of the WHO ExpertCommittee on the Control of Leishmaniases. **World Health Organization. Geneva.2010.**
2- ORGANIZACIÓN PANAMERICANA DE LA SALUD.**Leishmaniasis En Las Américas Recomendaciones Para El Tratamiento.** Washington, DC, 2013.
3- BRASIL, Ministério da Saúde. Secretaria de Vigilância em Saúde**. Manual de Vigilância da Leishmaniose Tegumentar Americana.** 2. ed. Brasília : Editora do Ministério da Saúde, 2010.
4- GONTIJO, Bernardo; CARVALHO, Maria de Lourdes Ribeiro de.Leishmaniose tegumentar americana**. Revista da Sociedade Brasileira de Medicina Tropical,** 36(1):71-80. Jan-fev, 2003. Disponível em: <http://scielo.br/pdf/rsbmt/v36n1/15310.pdf>
5- **WHO.** Global Health Observatory (GHO) data**.Wolrd health Organization. 2016.**
6- TEIXEIRA, D. E.; et al. **Atlas didático Ciclo de vida da *Leishmania*.**: Fundação CECIERJ, Consórcio CEDERJ, Rio de Janeiro, 2013.
7- KAYE, Paul; SCOTT, Phillip. Leishmaniasis: complexity at the host–pathogen Interface.**Nature Reviews,** Microbiology, v. 9, p.604-615,Aug. 2011. Disponível em <https://www.ncbi.nlm.nih.gov/pubmed/21747391>
8- DANTAS, Marina Loyola. **Aspectos Comparativos Da Resposta Inflamatória Em Lesões De Leishmaniose Cutânea Localizada e Disseminada.** 2012. 94 f. Dissertação (Mestrado em Patologia Humana) Faculdade de Medicina, Universidade Federal das Bahia, Salvador, 2012
9- DAVID, Consuelo V.; CRAFT, Noah.Cutaneous and mucocutaneous leishmaniasis**.Dermatologic Therapy**, v. 22, p. 491–502, Nov. 2009. Disponível em <https://www.ncbi.nlm.nih.gov/pubmed/19889134>.
10- PROGRAMA DE ZOONOSES REGIÃO SUL. **Manual de Zoonoses**. v.1, 2.ed, 2010
11 –VOULES, Dimitrios Alexios Karagiannis; et al. Bayesian Geostatistical Modeling of Leishmaniasis Incidence in Brazil**. PLoS Negl Trop Dis,** 7(5): e2213. May. 2013. Disponível em <https://www.ncbi.nlm.nih.gov/pmc/articles/PMC3649962/>.
12- Sistema Nacional de Agravos de Notificação (SINAN), Ministério da Saúde http://portalsaude.saude.gov.br/images/pdf/2016/novembro/08/LV-Casos.pdf http://portalsaude.saude.gov.br/images/pdf/2016/novembro/07/LT-Casos.pdf
13- CAMARGO, Luis M. Aranha; BARCINSKI, Marcello André. Leishmanioses, feridas bravas e kalazar. Cienc. Cult, v.55 no.1 São Paulo. Jan./Mar 2003. Disponível em <http://cienciaecultura.bvs.br/scielo.php?pid=S0009-67252003000100023&script=sci_arttext>
14- Galati EBA. Morfologia e Taxonomia. In: Rangel EF, Laison R, Flebotomídeos do Brasil. Rio de Janeiro: Fio Cruz; 2003 p.23-51
15- CARNEIRO, Andréa Lisbôa. Uso de terapia fotodinâmica com ftalocianina cloro alumínio no tratamento tópico da leishmaniose cutânea. 2013. Disponível em: <http://repositorio.unb.br/handle/10482/13954>
16- SANTAREM, N. et al. Immune response regulation by leishmania secreted and nonsecreted antigens. **J Biomed Biotechnol**, v. 2007, n. 6, p. 85154, 2007.ISSN 1110-7243. Disponível em: < http://www.ncbi.nlm.nih.gov/pubmed/17710243 >
17- MOAL, Vanessa Liévin-Le; LOISEAU, Philippe M. *Leishmania* hijacking of the macrophage intracelular compartments. **FEBS Journal**, v. 283, p. 598–607. Feb, 2015. Disponível em: <https://www.ncbi.nlm.nih.gov/pubmed/26588037>

18- RITTIG, M.G.; BOGDAN, C. Leishmania–Host-cell Interaction: Complexities and Alternative Views. Parasitology Today, v. 16, p. 292–297. July, 2000. Disponível em: <https://www.ncbi.nlm.nih.gov/pubmed/10858648>
19- DANTAS, Marina Loyola. **Aspectos Comparativos Da Resposta Inflamatória Em Lesões De Leishmaniose Cutânea Localizada e Disseminada.** 2012. 94 f. Dissertação (Mestrado em Patologia Humana) Faculdade de Medicina, Universidade Federal das Bahia, Salvador, 2012
20- VON STEBUT, E. Cutaneous Leishmania infection: progress in pathogenesis research and experimental therapy**. Exp Dermatol**, v. 16, n. 4, p. 340-6, Apr 2007. ISSN 0906-6705.Disponível em: <http://www.ncbi.nlm.nih.gov/pubmed/17359341>.
21- SANTAREM, N. et al. Immune response regulation by leishmania secreted and nonsecreted antigens.**J Biomed Biotechnol**, v. 2007, n. 6, p. 85154, 2007.ISSN 1110-7243. Disponível em: <http://www.ncbi.nlm.nih.gov/pubmed/17710243>.
22- ANTONELLI, L. R. et al. Antigen specific correlations of cellular immune responses in human leishmaniasis suggests mechanisms for immunoregulation. **Clin Exp Immunol**, v. 136, n. 2, p.341-8, May 2004.ISSN 0009-9104. Disponível em: <http://www.ncbi.nlm.nih.gov/pubmed/15086400>
23- BOGDAN, C.; RÖLLINGHOFF, M. The immune response to Leishmania: mechanisms of parasite control and evasion. **International Journal for Parasitology**, v. 24 - 28F, p. 121-134, 1998.LI, J.; Disponível em: <http://www.sciencedirect.com/science/article/pii/S0020751997001690>
24- HUNTER, C. A.; FARRELL, J. P. Anti-TGF-Treatment Promotes Rapid Healing of Leishmania major Infection in Mice by Enhancing In Vivo Nitric Oxide Production. **The Journal of Immunology** 1999. Disponível em: <http://www.jimmunol.org/content/162/2/974.short>
25- RITTIG, M.G.; BOGDAN, C. Leishmania–Host-cell Interaction: Complexities and Alternative Views**.Parasitology Today**, v. 16, p. 292–297. July, 2000. Disponível em: <https://www.ncbi.nlm.nih.gov/pubmed/10858648>
26- MOAL, Vanessa Liévin-Le; LOISEAU, Philippe M.*Leishmania* hijacking of the macrophage intracelular compartments.FEBS Journal, v. 283, p. 598–607. Feb, 2015. Disponível em: <https://www.ncbi.nlm.nih.gov/pubmed/26588037>
27- HANDMAN, Emanuela; BULLEN, Denise V. R. Interaction of *Leishmania* with the host macrophage**.Trends in Parasitology.** v.18 No.8, p. 332–334. Aug, 2002. Disponível em: <https://www.ncbi.nlm.nih.gov/pubmed/12377273>
28- LACERDA, Ariani F. et al. Anti-parasitic Peptides from Arthropods and their Application in Drug Therapy**.Frontiers in Microbiology**. v. 7. Article 91. February, 2016. Disponível em: <https://www.ncbi.nlm.nih.gov/pubmed/26903970>
29- BELAZ, Sorya; et al. Identification, biochemical characterization, and *in-vivo* expression of the intracellular invertase BfrA from the pathogenic parasite *Leishmania major***. Carbohydrate Research**. V. 415, p. 31–38. Oct, 2015. Disponível em: <https://www.ncbi.nlm.nih.gov/pubmed/26279524>
30- DUTHIE, Malcolm S. et al. The development and clinical evaluation of second-generation leishmaniasis vaccines.**Vaccine,** v. 30, n. 2, p. 134-41. Jan 5 2012. ISSN 1873-2518. Disponível em: <https://www.ncbi.nlm.nih.gov/pmc/articles/PMC3359766/>
31- COSTA, Inez Silva Fernandes. **Ação da molécula doadora de óxido nítrico S-Nitrosoglutationa (GSNO) na leishmaniose cutânea experimental.** 2007. 32 f. Dissertação (Mestrado em Imunologia) Instituto de Ciências Biomédicas, USP, São Paulo, 2007

32- VEGA, Jorge Humberto Pérez; et al. Leishmaniasis cutánea causada por Leishmania mexicana en Durango, México. Informe del primer caso clínico. **Gaceta médica de México**. v. 145 nº 5, p. 433-435, 2009. Disponível em: <https://dialnet.unirioja.es/servlet/articulo?codigo=4731345>
33- HALDAR, Arun Kumar; SEN, Pradip; ROY, Syamal. Use of antimony in the treatment of leishmaniasis: current status and future directions. **Mol Biol Int,** v. 2011, p. 571242, 2011. ISSN 2090-2190. Disponível em: <https://www.ncbi.nlm.nih.gov/pubmed/22091408>
34- BACON, Kristina M. et al. The potential economic value of a cutaneous leishmaniasis vaccine in seven endemic countries in the Americas.**Vaccine,** v. 31, n. 3, p. 480-6, Jan 7 2013. ISSN 1873-2518. Disponível em: <http://www.ncbi.nlm.nih.gov/pubmed/23176979>
35- WORKING GROUP ON RESEARCH PRIORITIES FOR DEVELOPMENT OF LEISHMANIASIS, V. et al. Vaccines for the leishmaniases: proposals for a research agenda. **PLoS Negl Trop Dis,** v. 5, n. 3, p. e943, 2011. ISSN 1935-2735. Disponível em: <http://www.ncbi.nlm.nih.gov/pubmed/21468307>
36- MURRAY, H. W. Leishmaniasis in the United States: treatment in 2012. Am J Trop Med Hyg, v. 86, n. 3, p. 434-40, Mar 2012. ISSN 1476-1645. Disponível em: <http://www.ncbi.nlm.nih.gov/pubmed/22403313>
37- SUNDAR, S. et al. Visceral leishmaniasis - current therapeutic modalities**.Indian J. Med. Res,** v. 123, p. 345-352. March, 2006. Disponível em: <https://www.ncbi.nlm.nih.gov/pubmed/16778315>
38- MCGWIRE, B.S.; SATOSKAR, A.R. Leishmaniasis: clinical syndromes and treatment**. Q J Med**. v. 107(1), p. 7–14. Jun, 2014. Disponível em: <https://www.ncbi.nlm.nih.gov/pubmed/23744570>
39- Sundar, Shyam; et al. Comparison of short-course multidrug treatment with standard therapy for visceral leishmaniasis in India:an open-label, non-inferiority, randomised controlled trial**. The Lancet**. v. 377 nº 9764, p. 477-486. Feb 5, 2011. Disponível em <https://www.ncbi.nlm.nih.gov/pubmed/21255828>
40- SANTOS, Jussamara B. et al**.** Antimony plus Recombinant Human Granulocyte-Macrophage Colony-Stimulating Factor Applied Topically in Low Doses Enhances Healing of Cutaneous Leishmaniasis Ulcers: A Randomized, Double-Blind, Placebo-Controlled Study**. The Journal of Infectious Diseases**, v.190, p.1793–6. Oct, 2004. Disponível em: <https://www.ncbi.nlm.nih.gov/pubmed/15499535>
41- ALMEIDA, R. et al. Randomized, Double-Blind Study of Stibogluconate Plus Human Granulocyte Macrophage Colony-Stimulating Factor versus Stibogluconate Alone in the Treatment of Cutaneous Leishmaniasis. **The Journal of Infectious Diseases** 1999;180:1735–7.
42- HAMMOND, David J.; GUTTERIDGE, Winston E. Purine And Pyrimidine Metabolism In The Trypanosomatidae. **Molecular and Biochemical Parasitology.** v. 13, p. 243-261. Nov, 1984. Disponível em: <http://www.sciencedirect.com/science/article/pii/0166685184901178>
43- MARR, J. J. et al. Purine Metabolism In Leishmania Donovani And*Leishmania braziliensis***. Biochimica et Biophysica Acta**, 544, 360—371. 1978.Disponível em: <https://www.ncbi.nlm.nih.gov/pubmed/719006>
44- CUSHNAN, D.W. et al. Rational Desing and Biochemical Utility of Specific Inhibitor of Angiotensin-Converting Enzyme. **Journal of Cardiovascular Pharmacology**.(Suppl. 7):S17-S30. New York. 1987. Disponível em: <http://journals.lww.com/cardiovascularpharm/Abstract/1987/06107/Rational_Design_and_Biochemical_Utility_of.4.aspx>

45- KOUNI, M. H. Potential chemotherapeutic targets in the purine metabolism of parasites**. Pharmacology & Therapeutics** 99, 283– 309. 2003. Disponível em: <http://www.sciencedirect.com/science/article/pii/S0163725803000718>
46- DUCATI, RG. et al. Purine salvage pathway in Mycobacterium tuberculosis. **Current medicinal chemistry**, v. 18, n. 9, p. 1258-1275, 2011. Disponível em: <http://www.ingentaconnect.com/content/ben/cmc/2011/00000018/00000009/art00002>
47- BERENS, R.L. et al. Purine and Pyramidine Metabolism**.** Biochemistry and Molecular Biology of Parasites.P.89-117. **Academic Press Ltda**. 1995. Disponível em: <https://books.google.com.br/books?hl=pt-BR&lr=&id=8w_hXAW5JCYC&oi=fnd&pg=PP2&dq=Purine+and+Pyramidine+Metabolism.+Biochemistry+and+Molecular+Biology+of+Parasites&ots=olxq7xSciy&sig=ckxmzL1yaCHvZCDxM11yylu0I_0#v=onepage&q=Purine%20and%20Pyramidine%20Metabolism.%20Biochemistry%20and%20Molecular%20Biology%20of%20Parasites&f=false>
48- HAMMOND, David J.; GUTTERIDGE, Winston E. Purine And Pyrimidine Metabolism In The Trypanosomatidae. **Molecular and Biochemical Parasitology.** v. 13, p. 243-261. Nov, 1984. Disponível em: <http://www.sciencedirect.com/science/article/pii/0166685184901178>
49- Voet, D. and Voet, J. G. **Bioquímica.** Cap. 28, p. 1113-1120. 3ª Ed. Panamericana. 2006 50 –Stryer, L. **Biohemistry.** Cp. 25, p. 495-501. 4ª Ed. Guanabara Koogan S.A. 1992.
50- LAFON, Stephen W. et al. Purine and pyrimidine salvage pathways in Leishmania donovani. **Biochemical pharmacology**, v. 31, n. 2, p. 231-238, 1982. Disponível em: <http://www.sciencedirect.com/science/article/pii/0006295282902167>
51- Vierira, E. C. et al. **Biologia celular e biologia molecular**. Cap. 16, p 261-270. 2ª Ed. Atheneu. 1999.
52- LINSTEAD, David. New defined and semi-defined media for cultivation of the flagellate *Trichomonas vaginalis.* **Parasitology.** v.3, p. 125-137. Aug, 1981. Disponível em: <https://www.ncbi.nlm.nih.gov/pubmed/6973740>.
53- BRUN, R; SCHONENBERGER, M. Cultivation and in 'vitro cloning of procyclic culture forms of *Trypanosoma brucei* in a semi-defined medium**. Acta Trop**. v. 36(3), p. 289-292, 1979. Disponível em:
54- KIDDER, G.W.; DUTTA, B.N. The growth and nutrition of *Crithidia fasciculata.***J. Gen. Microbiol**. v. 18, p. 621-638, 1958. Disponível em: <http://www.microbiologyresearch.org/docserver/fulltext/micro/18/3/mic-18-3-621.pdf?expires=1483893529&id=id&accname=guest&checksum=D994F0F29C4AAFFEB609FD797A391390>
55- TRAGER, William. Nutrition and biosynthetic capabilities of flagellates: problems of in vitro cultivation and differentiation. In: **Ciba Foundation Symposium 20-Trypanosomiasis and Leishmaniasis (with Special Reference to Chagas' Disease)**. John Wiley & Sons, Ltd., 1974. p. 225-254. Disponível em: <http://onlinelibrary.wiley.com/doi/10.1002/9780470720035.ch12/summary>
56- MELO, Norma Maria; DE AZEVEDO, H. P.; ROITMAN, I.; MAYRINK, W. A new defined medium for cultivating *Leishmania* promastigotes.**Acta Trop**. v. 42, p. 137-141. July, 1985. Disponível em: <http://cat.inist.fr/?aModele=afficheN&cpsidt=8398074>
57- STEIGER, ROLF F.; STEIGER, Erica. Cultivation of *Leishmania donovani and Leishmania braziliensis* in defined medium: nutritional requirements. **J. Protozool**. v.

24, p. 437-441. Aug, 1977. Disponível em: <http://onlinelibrary.wiley.com/doi/10.1111/j.1550-7408.1977.tb04771.x/abstract>
58- LAFON, Stephen W. et al. Purine and pyrmide salvage pathways in Leishmania donovani. **Biochem Pharmacol.** v. 31, p.231-238. Jan, 1982. Disponível em: <https://www.ncbi.nlm.nih.gov/pubmed/7059364>
59- CUI, L.; RAJASEKARIAH, G.R; MARTIN S.K. A nonspecific nucleoside hydrolase from leishmania dnovovani: implications for purine salvage by the parasite. **Gene** v.280, p. 153-162. Dec, 2001 Disponível em: <https://www.ncbi.nlm.nih.gov/pubmed/11738828>
60- BOITZ, Jan M. et al. Purine salvage in leishmania: complex or single by design? **Trends Parasito**. v. 28 p. 345-352. Ayg, 2012. Disponível em: <https://www.ncbi.nlm.nih.gov/pubmed/22726696>
61- IOVANE, E. et al. Structural basis for substrate specificity in grupo l nucleoside hydrolases. **Biochemistry**. v. 47 p. 4418-4426. Fev, 2008.
62- PARKIN, David W. et al. Nucleoside hydrolase from Crithidia fasciculata. Metabolic role, purification, specificity, and kinetic mechanism. **Journal of Biological Chemistry**, v. 266, n. 31, p. 20658-20665, 1991. Disponível em: <http://www.jbc.org/content/266/31/20658.short>
63- PARKIN, David W.; SCHRAMM, Vern L. Binding modes for substrate and a proposed transition-state analog of protozoan nucleoside hydrolase. **Biochemistry**, v. 34, n. 42, p. 13961-13966, 1995. Disponível em: <http://pubs.acs.org/doi/abs/10.1021/bi00042a030?journalCode=bichaw>
64- PARKIN, David W. Purine-specific nucleoside N-ribohydrolase from Trypanosoma brucei purification, specificity, and kinetic mechanism. **Journal of Biological Chemistry**, v. 271, n. 36, p. 21713-21719, 1996. Disponível em: <http://www.jbc.org/content/271/36/21713.short>
65- SHI, Wuxian; SCHRAMM, Vern L.; ALMO, Steven C. Nucleoside hydrolase from Leishmania major Cloning, expression, catalytic properties, transition state inhibitors, and the 2.5-Å crystal structure. **Journal of Biological Chemistry**, v. 274, n. 30, p. 21114-21120, 1999. Disponível em: <http://www.jbc.org/content/274/30/21114.short>
66- PETERSEN, Carsten; MØLLER, Lisbeth Birk. The RihA, RihB, and RihC Ribonucleoside Hydrolases ofEscherichia coli SUBSTRATE SPECIFICITY, GENE EXPRESSION, AND REGULATION. **Journal of Biological Chemistry**, v. 276, n. 2, p. 884-894, 2001. Disponível em: < http://www.jbc.org/content/276/2/884.short>
67- OGAWA, Jun et al. Purification, characterization, and gene cloning of purine nucleosidase from Ochrobactrum anthropi. **Applied and environmental microbiology**, v. 67, n. 4, p. 1783-1787, 2001. Disponível em: <http://aem.asm.org/content/67/4/1783.short>
68- RIBEIRO, José MC; VALENZUELA, Jesus G. The salivary purine nucleosidase of the mosquito, Aedes aegypti. **Insect biochemistry and molecular biology**, v. 33, n. 1, p. 13-22, 2003. Disponível em: <http://www.sciencedirect.com/science/article/pii/S0965174802000784>
69- DEGANO, Massimo et al. Trypanosomal nucleoside hydrolase. A novel mechanism from the structure with a transition-state inhibitor. **Biochemistry**, v. 37, n. 18, p. 6277-6285, 1998. Disponível em: <http://pubs.acs.org/doi/abs/10.1021/bi973012e>
70- VERSÉES, W. et al. Structure and function of a novel purine specific nucleoside hydrolase from Trypanosoma vivax. **Journal of molecular biology**, v. 307, n. 5, p. 1363-1379, 2001. Diisponivel em: <http://www.sciencedirect.com/science/article/pii/S0022283601945486>

71- KOSZALKA, George Walter; KRENITSKY, T. A. Nucleosidases from Leishmania donovani. Pyrimidine ribonucleosidase, purine ribonucleosidase, and a novel purine 2'-deoxyribonucleosidase. **Journal of Biological Chemistry**, v. 254, n. 17, p. 8185-8193, 1979.
72- ESTUPIÑÁN, Bernardo; SCHRAMM, Vern L. Guanosine-inosine-preferring nucleoside N-glycohydrolase from Crithidia fasciculata. **Journal of Biological Chemistry**, v. 269, n. 37, p. 23068-23073, 1994. Disponível em: <http://www.jbc.org/content/269/37/23068.short>
73- FIGUEROA-VILLAR, José D.; SALES, Edijane M. The importance of nucleoside hydrolase enzyme (NH) in studies to treatment of Leishmania: A review. **Chemico-Biological Interactions**, 2016. Disponível em: <http://www.sciencedirect.com/science/article/pii/S0009279716306731>
74- MAZZELLA, L. John et al. Mechanistic diagnoses of N-ribohydrolases and purine nucleoside phosphorylase. **Journal of the American Chemical Society**, v. 118, n. 8, p. 2111-2112, 1996. Disponível em: <http://pubs.acs.org/doi/abs/10.1021/ja953537z?journalCode=jacsat>
75- GOPAUL, Deshmukh N. et al. Inosine− Uridine Nucleoside Hydrolase from Crithidia fasciculata. Genetic Characterization, Crystallization, and Identification of Histidine 241 as a Catalytic Site Residue†. **Biochemistry**, v. 35, n. 19, p. 5963-5970, 1996. Disponível em: <http://pubs.acs.org/doi/abs/10.1021/bi952998u>
76- HORENSTEIN, Benjamin A. et al. Transition-state analysis of nucleoside hydrolase from Crithidia fasciculata. **Biochemistry**, v. 30, n. 44, p. 10788-10795, 1991. Disponível em: <http://pubs.acs.org/doi/abs/10.1021/bi00079a004?journalCode=bichaw>
77- HORENSTEIN, Benjamin A.; SCHRAMM, Vern L. Electronic nature of the transition state for nucleoside hydrolase. A blueprint for inhibitor design. **Biochemistry**, v. 32, n. 28, p. 7089-7097, 1993. Disponível em: <http://pubs.acs.org/doi/abs/10.1021/bi00079a004?journalCode=bichaw>
78- FREITAS, Elisangela Oliveira et al. Immucillins ImmA and ImmH are effective and non-toxic in the treatment of experimental visceral leishmaniasis. **PLoS Negl Trop Dis**, v. 9, n. 12, p. e0004297, 2015. Disponível em: <https://www.ncbi.nlm.nih.gov/pubmed/25909893>

Pontifícia Universidade Católica do Rio Grande do Sul
Pró-Reitoria de Graduação
Av. Ipiranga, 6681 - Prédio 1 - 3º. andar
Porto Alegre - RS - Brasil
Fone: (51) 3320-3500 - Fax: (51) 3339-1564
E-mail: prograd@pucrs.br
Site: www.pucrs.br